Mammalian bone palaeohistology: new data and a survey

Christian Kolb, Torsten M. Scheyer, Kristof Veitschegger, Analia M. Forasiepi, Eli Amson, Alexandra van der Geer, Lars W. van den Hoek Ostende, Shoji Hayashi, Marcelo R. Sánchez-Villagra

The interest in mammalian palaeohistology has increased dramatically in the last two decades. Starting in 1849 via descriptive approaches, it has been demonstrated that bone tissue and vascularisation types correlate with several biological variables such as ontogenetic stage, growth rate, and ecology. Mammalian bone displays a large variety of bone tissues and vascularisation patterns reaching from lamellar or parallel-fibred to fibrolamellar or woven-fibred bone, depending on taxon and individual age. Here we systematically review the knowledge and methods on mammalian bone and palaeohistology and discuss potential future research fields and techniques. We present new data on the bone microstructure of two extant marsupial species and of several extinct continental and island placental mammals. Three juvenile specimens of the dwarf island hippopotamid *Hippopotamus minor* from the Late Pleistocene of Cyprus show reticular to plexiform fibrolamellar bone. The island murid *Mikrotia magna* from the Late Miocene of Gargano, Italy displays parallel-fibred primary bone with reticular vascularisation being pervaded by irregular secondary osteons in the central part of the cortex. *Leithia* sp., the dormouse from the Pleistocene of Sicily, is characterised by a primary bone cortex consisting of lamellar bone and low vascularisation. The bone cortex of the fossil continental lagomorph *Prolagus oeningensis* and three fossil species of insular *Prolagus* displays parallel-fibred primary bone and reticular, radial as well as longitudinal vascularisation. Typical for large mammals, secondary bone in the giant rhinocerotoid *Paraceratherium* sp. from the Miocene of Turkey is represented by dense Haversian bone. The skeletochronological features of *Sinomegaceros yabei*, a large-sized deer from the Pleistocene of Japan closely related to *Megaloceros*, indicate a high growth rate. These examples and the critical summary of existing data show how bone microstructure can reveal essential information on life history evolution. The bone tissue and the skeletochronological data of the sampled island species show that there is no universal modification of bone tissue and life history specific to insular species.

Mammalian bone palaeohistology: new data and a survey

Christian Kolb[1*], Torsten M. Scheyer[1], Kristof Veitschegger[1], Analia M. Forasiepi[2], Eli Amson[1], Alexandra van der Geer[3], Lars W. van den Hoek Ostende[3], Shoji Hayashi[4], Marcelo R. Sánchez-Villagra[1]

[1]*Paläontologisches Institut und Museum der Universität Zürich, Karl Schmid-Strasse 4, CH-8006 Zürich, Switzerland (christian.kolb@pim.uzh.ch, Tel. +41(0)446342269; tscheyer@pim.uzh.ch, Tel.: +41(0)446342322; kristof.veitschegger@pim.uzh.ch, Tel.: +41(0)446342329; eli.amson@pim.uzh.ch, Tel +41(0)446342148; m.sanchez@pim.uzh.ch, Tel. +41(0)446342342)*

[2] *Consejo Nacional de Investigaciones Científicas y Técnicas (CONICET), Instituto Argentino de Nivología, Glaciología y Ciencias Ambientales (IANIGLA), Centro Científico y Tecnológico (CCT), Av. Ruiz Leal s/nº 5500, Mendoza-ciudad, Mendoza, Argentina (acanthodes@gmail.com, Tel. +54(261)5244253)*

[3] *Naturalis Biodiversity Center, P.O. Box 9517, 2300 RA Leiden, The Netherlands (alexandra.vandergeer@naturalis.nl, Tel. +31(0)717517390; lars.vandenhoekostende@naturalis.nl, Tel.* +31(0)715687685*)*

[4] *Osaka Museum of Natural History, Nagai Park 1-23, Higashi-Sumiyoshi-Ku, Osaka, 546-0034, Japan (hayashi@mus-nh.city.osaka.jp)*

*Corresponding author

Abstract

The interest in mammalian palaeohistology has increased dramatically in the last two decades. Starting in 1849 via descriptive approaches, it has been demonstrated that bone tissue and vascularisation types correlate with several biological variables such as ontogenetic stage, growth rate, and ecology. Mammalian bone displays a large variety of bone tissues and vascularisation patterns reaching from lamellar or parallel-fibred to fibrolamellar or woven-fibred bone, depending on taxon and individual age. Here we systematically review the knowledge and methods on mammalian bone and palaeohistology and discuss potential future research fields and techniques. We present new data on the bone microstructure of two extant marsupial species and of several extinct continental and island placental mammals. Three juvenile specimens of the dwarf island hippopotamid *Hippopotamus minor* from the Late Pleistocene of Cyprus show reticular to plexiform fibrolamellar bone. The island murid *Mikrotia magna* from the Late Miocene of Gargano, Italy displays parallel-fibred primary bone with reticular vascularisation being pervaded by irregular secondary osteons in the central part of the cortex. *Leithia* sp., the dormouse from the Pleistocene of Sicily, is characterised by a primary bone cortex consisting of lamellar bone and low vascularisation. The bone cortex of the fossil continental lagomorph *Prolagus oeningensis* and three fossil species of insular *Prolagus* displays parallel-fibred primary bone and reticular, radial as well as longitudinal vascularisation. Typical for large mammals, secondary bone in the giant rhinocerotoid *Paraceratherium* sp. from the Miocene of Turkey is represented by dense Haversian bone. The skeletochronological features of *Sinomegaceros yabei*, a large-sized deer from the Pleistocene of Japan closely related to

Megaloceros, indicate a high growth rate. These examples and the critical summary of existing data show how bone microstructure can reveal essential information on life history evolution. The bone tissue and the skeletochronological data of the sampled island species show that there is no universal modification of bone tissue and life history specific to insular species.

Introduction

Histology of fossil bones (e.g. Ricqlès, 1976a; Padian, 2011) provides data to investigate life history variables such as age, sexual maturity, growth patterns, and reproductive cycles. Research on fossil vertebrate hard tissues dates back to the 19th century when it was recognised that bones and teeth are commonly very well preserved at the histological level (Quekett, 1849a; Quekett, 1849b). Since then, several descriptive surveys of different tetrapod taxa, including mammals, were published (e.g. Schaffer, 1890; Enlow & Brown, 1958; Ricqlès, 1976a; Ricqlès, 1976b; Klevezal, 1996; Marin-Moratalla et al., 2014; Prondvai et al., 2014). The study of the microstructure of highly mineralised components such as blood vessel arrangement (de Boef & Larsson, 2007) and tissue types in bones as well as teeth (e.g. Kolb et al., 2015) provides information on growth patterns and remodelling processes of hard tissues in extinct vertebrates (see also Scheyer, Klein & Sander, 2010; Chinsamy-Turan, 2012a; and Padian & Lamm, 2013 for summaries).

Mammals are a well-known group of vertebrates with a well-documented fossil record. However, until recent years and apart from a few seminal papers (Gross, 1934; Enlow & Brown, 1958; Warren, 1963; Klevezal, 1996), mammalian bone histology received little attention by biologists and palaeontologists alike compared to dinosaurs and non-mammalian synapsids (e.g.

Horner, Ricqlès & Padian, 1999; Sander et al., 2004; Chinsamy-Turan, 2012; see also Padian, 2013 for a review on Chinsamy-Turan, 2012a).

The present contribution summarizes the main aspects about the current state of knowledge on mammalian palaeohistology, presents new finds on several extant and extinct species from diverse clades, and discusses perspectives in this field of research. Literature dealing with pathologies in mammalian bone is omitted since this would go beyond the scope of this synthesis.

Bone tissue types

Bone is composed of an organic phase and an anorganic mineral phase consisting of carbonate hydroxyl apatite —$Ca_{10}(PO_4\ Ca_3)_6(OH)_2$. Being a complex and specialized ~~connective~~ tissue, bone, along with cartilage, forms the skeleton of all tetrapods. During fossilization, the hydroxyl group as part of the anorganic bone phase is replaced by fluorine to form carbonate fluorapatite, while the organic component, consisting mainly of Type I collagen, usually decomposes. However, the more resistant anorganic (mineral) component of the bone is only prone to minor changes and still depicts the original microstructure (Francillon-Vieillot et al., 1990; Chinsamy-Turan, 2012).

In mammals, three main types of bone matrix are distinguished. *Woven-fibred bone* shows very low spatial arrangement. It consists of highly disorganised collagen fibres of different sizes being loosely and randomly arranged. *Parallel-fibred bone* consists of tightly packed collagen fibrils arranged in parallel. *Lamellar bone* shows the highest spatial organisation. It consists of thin layers (lamellae) of closely packed collagen fibres. Both parallel-fibred and lamellar bone are indicative of relatively low growth rates (Francillon-Vieillot et al.,

1990; Huttenlocker , Woodward & Hall, 2013). Bromage et al. (2009) confirmed that lamellar bone is an incremental tissue, with one lamella formed in the species-specific time dependency of the formation of long-period increments (striae of Retzius) in enamel. The authors showed as well a negative correlation between osteocyte density in bone and body mass and therefore suggested a central autonomic regulatory control mechanism to the coordination of organismal life history and body mass.

A bone complex composed of woven-fibred scaffolding and intervening primary osteons of varying orientations, i.e. parallel-fibred or lamellar bone, is defined as *fibrolamellar bone* (Figs. 1B, 1C, 1E, 1F) (Ricqlès, 1974a) or fibrolamellar complex (FLC; Ricqlès et al., 1991; Margerie, Cubo & Castanet, 2002). According to its vascular orientation, three main types of fibrolamellar bone are distinguished: *Laminar bone* shows an almost uniform circumferential orientation of vascular canals. In case ~~inar~~ canals are connected by radial ones forming a dense anastomosing network, the pattern is called *plexiform* (Figs. 1B, 1C, 1E, 1F). An anastomosing network showing random organisation with oblique orientations is defined as reticular. Moreover, a radial arrangement of vascular canals is called *radiating* or *radial bone* (Francillon-Vieillot et al., 1990; Chinsamy-Turan, 2012b; Huttenlocker, Woodward & Hall, 2013).

An ho identified for the first time a relationship between bone tissue type and growth rate in vertebrates, what is now called Amprino's rule (Amprino, 1947). This was a milestone for the development of a modern biological approach in palaeohistology, and was tested in several studies on extant birds (Castanet et al., 2000; Margerie, Cubo & Castanet, 2002; Margerie et al., 2004). He observed that in slow growing animals or animals in late stages of ontogeny, periosteal bone is generally denser, less vascularised, and shows higher spatial arrangement. By

contrast, in fast growing animals such as mammals or in juveniles, periosteal bone is less dense and more vascularised with a high number of primary osteons, which in turn become embedded in a matrix of parallel-fibred or lamellar bone, constituting what was originally called the fibrolamellar complex by Ricqlès (1975) and subsequent authors (e.g. Köhler & Moyà-Solà, 2009; Marin-Moratalla, Jordana & Köhler, 2013). Later studies also demonstrated a relationship between periosteal growth rate and pattern of vascularisation, i.e. that growth is positively correlated with the degree of radially organised vascularisation (Margerie et al., 2004; see also Lee et al., 2013).

Stein & Prondvai (2013) found, by investigating longitudinal thin sections of sauropod long bones, that the amount of woven bone in the primary complex has been largely overestimated (e.g., Klein & Sander 2008), questioning former arguments on the biology and life history of sauropod dinosaurs. Similarly, Kolb et al. (2015) showed, via longitudinal thin sections, that in the giant deer *Megaloceros giganteus* the amount of woven-fibred bone within the fibrolamellar complex (FLC) is easily overestimated as well.

Growth marks and skeletochronology

Different types of growth marks in the bone cortex are distinguished in the osteohistological literature. They are deposited cyclically, usually occurring within lamellar or parallel-fibred bone. All kinds of growth marks indicate a change in growth rate or a complete arrest of growth.

Growth zones can be composed of any bone type or vascular pattern and represent a period of relatively elevated growth rate. *Annuli* indicate a period of relatively slower growth and consist of parallel-fibred or lamellar bone. *Lines of arrested growth* (LAGs) are thin,

139 semitranslucent to opaque bands (Huttenlocker, Woodward & Hall, 2013) under linear or crossed
140 polarised light indicating a complete cessation of growth. In case they have not been obliterated
141 by bone resorption or remodelling processes, they appear as thin and almost or completely
142 opaque bands and comprise the whole circumference of the bone cortex. In all groups of
143 mammals, except those reaching skeletal maturity within their first year of life, lines of arrested
144 growth occur (Morris, 1970; Frylestam & Schantz, 1977; Buffrenil, 1982; Chinsamy, Rich &
145 Vickers-Rich, 1998; Klevezal, 1996; Castanet et al., 2004; Köhler et al., 2012). It has repeatedly
146 been confirmed and is now widely accepted that LAGs are deposited annually (e. g. Castanet &
147 Smirina, 1990; Buffrénil & Castanet, 2000; Castanet, 1994; Marangoni et al., 2009; Chinsamy-
148 Turan, 2012b) and independently of metabolic rate and climatic background (Köhler et al., 2012;
149 Huttenlocker, Woodward & Hall, 2013) and therefore they can be used for age estimations,
150 estimates of age at sexual or skeletal maturity, and growth rate analysis.

151 Castanet et al. (2004) studied LAGs in long bones, mandibles, and tooth cementum (M2
152 and M3) of captive specimens of known age of the mouse lemur, *Microcebus murinus*. The 43
153 male and 23 female specimens sampled ranged from juveniles to 11-year-old adults, for which
154 LAG counts and ages correlated best in the tibiae. In individuals older than seven years the
155 correlation decreased, leading to an age underestimation of three to four years and demonstrating
156 limitations of skeletochronology in long bones (Klevezal, 1996; Castanet, 2006). Additionally,
157 animals exposed to an artificially accelerated photoperiodic regimen (a 10-month cycle) show a
158 higher number of LAGs than animals of the same true age in which a yearly photoperiod is
159 maintained. According to that, there is strong evidence that photoperiodicity is an essential factor
160 for the deposition of LAGs rather than environmental factors (see also Woodward, Padian &
161 Lee, 2013).

Köhler et al. (2012) additionally demonstrated that the annual formation of LAGs is present throughout ruminants and that a cyclic arrest of growth in bone is mainly triggered by hormonal cues rather than environmental stresses. By confirming seasonal deposition of LAGs throughout ruminants, the general occurrence of LAGs in homeothermic endotherms has been confirmed, precluding the use of lines of arrested growth as an indicator of ectothermy.

Different kinds of processes in the cortex potentially remove parts of the growth record and may erase early LAGs. One of those processes is the substitution of primary bone tissue by secondary bone tissue in areas where resorption previously occurred. Secondary bone can appear as *Haversian bone* (Fig. 1I) consisting of clustered Haversian systems as a response to damage such as microcracks or around the medullary cavity forming endosteal lamellar bone as a response to ontogenetic changes in bone shape, i.e. bone drift (Enlow, 1962).

Several approaches to retrocalculate the lost information have been attempted and there are two ways of retrocalculating missing years. First, in case an appropriate ontogenetic growth series sampling is not available, it is possible to do arithmetic estimates of the missing intervals, done first for dinosaurs (e.g. Sander & Tückmantel, 2003; Horner & Padian, 2004; Erickson et al., 2004). The second approach is the superimposition of thin sections of long bones of different ontogenetic stages as, again done first for dinosaurs (e.g. Horner, Ricqlès & Padian, 2000; Bybee, Lee & Lamm, 2006; Lee & Werning, 2008; Erickson, 2014; see also Woodward, Padian & Lee, 2013 for more methodological details).

Marin-Moratalla, Jordana & Köhler (2013) were the first to apply the superimposition method to mammals using anteroposterior diameters of successive growth rings in five antelope (*Addax*) femora of different ages. They found that the first LAG in adult specimens fits the second growth cycle of juveniles, indicating that the first LAG is lost by resorption throughout

ontogeny. On one hand, this allowed estimates of age at death by counting all the rest lines in the bone cortex and increasing the LAG count by one. On the other hand, it was possible to estimate age at sexual maturity. When an animal becomes sexually or somatically mature, this is indicated by the deposition of a narrow layer of avascular lamellar bone, called the *outer circumferential layer* (OCL, Ponton et al., 2004; Figs. 1B, 1C), also referred to as the *external fundamental system* (EFS, *sensu* Horner, Ricqlès & Padian, 1999; see also Woodward, Padian & Lee, 2013). Given that Cormack (1987) uses the term "outer circumferential lamellae" (p. 305), we follow Ponton et al. (2004) in using the term outer circumferential layer (OCL) instead of EFS. Marin-Moratalla, Jordana & Köhler (2013) interpreted the transition from the FLC to the OCL to represent attainment of sexual maturity, since in the extant antelope *Addax* maturity estimates correlate well with individual tooth eruption and wear stages, as well as life history data. Therefore, the authors could show that in antelopes it is possible to determine age at sexual maturity and death. However, a recent study by Kolb et al. (2015) on fossil and extant cervids showed that the use of the OCL as a marker of sexual maturity can be misleading. Maturity estimates in extant cervids based on bone microstructure corresponded much more with the timing of the attainment of skeletal maturity, and, therefore, it represents skeletal rather than sexual maturity in cervids.

Material and methods

In order to contribute to a more complete picture of mammalian palaeohistology, long bones of the following additional mammalian taxa of which the bone histological characteristics are not or only poorly documented in the literature, including several taxa of extinct insular mammals, have been sampled (Table 1): The extant white-eared opossum *Didelphis albiventris*

and the thick-tailed opossum *Lutreolina crassicautada*, the giant deer *Megaloceros giganteus* from the Late Pleistocene of Ireland, the Asian giant deer *Sinomegaceros yabei* from the Late Pleistocene of Japan, the extant southern pudu *Pudu* puda, the Cyprus dwarf hippopotamid *Hippopotamus minor* from the Late Pleistocene of Cyprus, the dormouse *Leithia* sp. from the Pleistocene of Sicily, the giant hornless rhinocerotoid *Paraceratherium* sp. from the Late Oligocene of Turkey, the continental pika *Prolagus oeningensis* from the Middle Miocene of La Grive, France, and the Sardinian pika *Prolagus sardus* from the Late Pleistocene. From the Late Miocene of Gargano, Italy, the following material was sampled: The galericine insectivore *Deinogalerix* sp., the giant murid *Mikrotia magna*, as well as the giant pikas *Prolagus apricenicus* and *Prolagus imperialis*. Ontogenetic stages in long bones have been determined by the state of epiphyseal fusion (Habermehl, 1985).

Following standard procedures, bones were coated and impregnated with epoxy resin (Araldite or Technovit) prior to sawing and grinding. Long bones were transversely sectioned at mid-shaft where the growth record is most complete (e.g. Sander & Andrassy 2006; Kolb et al., 2015). Long bones of *Megaloceros giganteus* were also sampled by using a diamond-studded core drill, with sampled cores being subsequently processed (Sander & Andrassy, 2006; Stein & Sander, 2009). Sections were observed in normal transmitted and cross-polarised light using a Leica DM 2500 M composite microscope equipped with Leica DFC 420 C digital camera. Phylogenies have been produced using Mesquite 3.02© (Maddison & Maddison, 2015) and Adobe Illustrator CS5©.

Mammalian bone histology – works before 1935

The initial contribution on the bone palaeohistology of mammals was performed by Quekett (1849a, 1849b) as part of a comprehensive study dealing with the bone cortex of not only mammals but also fish, reptiles, and birds. He described mammalian long bone tissue comprising the fossil proboscidean *Mastodon*, the fossil xenarthran *Megatherium*, and humans to show Haversian canals, bony laminae, bone-cells, and canaliculi as well as a the typical three layered composition of cranial bones, ribs, and scapulae with two thin compact layers and one inner cancellous layer. Aeby (1878) concentrated on taphonomical aspects and compared bone tissue of reptiles, birds, and mammals. Kiprijanoff (1883) described in a comparative study of fossil material from Russia the bone cortex of *Bos primigenius*. Schaffer (1890) described the bone tissue of several mammalian taxa, including sirenians from the Eocene, Oligocene, and Miocene (*Halitherium*), a proboscidean from the Miocene (*Mastodon*), an undetermined fossil cetacean, and artiodactyls (an undetermined artiodactyl referred to an antelope and to *Hippopotamus*, both from the Pliocene). Schaffer also investigated Artiodactyla (*Sus scrofa,Capreolus*), Carnivora (*Ursus spelaeus*), Rodentia (*Arvicola*), as well as undetermined long and skull bones, all from the Pleistocene. Nopcsa and Heidsieck (1933) studied the bone tissue in ribs of dinosaurs, ichthyosaurs and therapsids (dicynodonts). Small individuals of *Dicynodon* and *Lystrosaurus* consist of “unlaminated” bone (p. 222) without secondary Haversian bone, whereas full-grown individuals exposed lamellar primary bone tissue with Haversian systems. Nopcsa and Heidsieck (1934) studied apart from reptile bones, ribs of sirenians (*Halitherium*). In his comparative work, Gross (1934) studied the bone cortex of a dicynodont (*Kannemeyeria*) and of the proboscidean *Mammuthus*.

Bone histology of extinct and extant synapsid clades

253 *Non-therapsid synapsids*- More than 320 Myr ago during the Carboniferous, reptilian-grade
254 amniotes and synapsids, the lineage leading to mammals including basal forms such as
255 edaphosaurids and sphenacodontids (Figs. 2, 3), diverged (Huttenlocker & Rega, 2012). Because
256 of their phylogenetic position, the understanding of the evolution and structure of their skeleton
257 is essential, since the anamniote-amniote transition was accompanied by the transition from a
258 mainly amphibious to a terrestrial biomechanical regime and life cycle (Romer, 1957; Romer,
259 1958; Germain & Laurin, 2005). In order to decipher essential life history parameters and
260 especially thermophysiology in basal synapsids, several authors studied the microstructure of
261 their long bones and neural spines comparing them to extant mammals and birds (Enlow &
262 Brown, 1957; Enlow & Brown 1958; Peabody, 1961; Warren, 1963; Ricqlès, 1974a; Ricqlès,
263 1976a; Bennett & Ruben, 1986). Cyclic and regularly lamellated ("lamellar-zonal") bone tissues
264 in early edaphosaurids and sphenacodontids revealed similarity in bone tissue type to extant
265 reptiles and amphibians (Ricqlès, 1974a; Ricqlès, 1974b; Ricqlès, 1976; Enlow, 1969).
266 Huttenlocker (2008) noted bone histological differences between sphenacodontids and
267 edaphosaurids. Sphenacodontids show fibrolamellar (see also Shelton et al., 2013) or parallel-
268 fibred bone, whereas edaphosaurids are mainly characterised by lamellar-zonal bone. In
269 conclusion, basal synapsids display a histological organisation that is suggestive of slow growth
270 (Huttenlocker & Rega, 2012). Peabody (1961) and Warren (1963) showed the occurrence and
271 skeletochronological relevance of growth marks in Palaeozoic synapsids, while Ricqlès (1969;
272 1972; 1974a; 1974b; 1975; 1976a; 1976b) studied several basal synapsid taxa in a series of
273 publications. Vickaryous and Sire (2009) reviewed the integumentary skeleton of tetrapods and
274 mentioned varanopid osteoderms to have a block-like morphology, organised into multiple
275 transverse rows in the cervical and pectoral regions. Bone compactness profiles are used in more

recent publications to infer habitat and ecology (e.g. Germain & Laurin, 2005; Kriloff et al., 2008). Growth and mechanics of unusual skeletal structures are discussed by Rega et al. (2005), Huttenlocker, Rega & Sumida (2010), and Huttenlocker, Mazierski & Reisz (2011). Laurin & Buffrénil (2015) studied the histology and compactness of ophiacodontid bone tissue. *Clepsydrops collettii*, a Late Carboniferous ophiacodontid, displayed a thin, compact cortex lacking a medullary spongiosa, therefore suggesting a terrestrial lifestyle. An optimisation of inferred lifestyle of other early stegocephalians (based on bone microanatomy) indicated that the first amniotes were terrestrial. The Early Permian *Ophiacodon uniformis* showed a thicker cortex with few resorption cavities and bone trabeculae surrounding the free medullary cavity, thus indicating a possibly secondary amphibious lifestyle. Shelton & Sander (2015) showed the existence of highly vascularised fibrolamellar bone in *Ophiacodon* by sampling an ontogenetic series of humeri and additional femora, and therefore providing evidence for fast skeletal growth. Hence, they suggested to set the evolutionary origin of modern mammalian endothermy and high skeletal growth rates back to the Early Permian.

Dicynodontia – A large amount of studies on therapsid histology deals with dicynodont long bones, cranial bones, and ribs. Early work on the bone histology of several dicynodont genera has been performed by Nopcsa & Heidsieck (1933), Gross (1934), Enlow & Brown (1957), Enlow (1969), Ricqlès (1972; 1975; 1976a). More recent work contributed essentially to a better understanding of general dicynodont histology, containing studies on isolated bones of several individuals, several skeletal elements of one individual or dicynodont biomechanics (e.g. Chinsamy & Rubidge, 1993; Ray & Chinsamy, 2004; Ray, Chinsamy & Bandyopadhyay, 2005; Green, Schweitzer & Lamm, 2010; Ray, Bandyopadhyay & Appana, 2010; Botha-Brink & Angielczyk, 2010; Botha-Brink & Angielczyk 2010; Jasinoski, Rayfield & Chinsamy, 2010a;

299 Jasinoski, Rayfield & Chinsamy, 2010b; Chinsamy-Turan, 2012b; Nasterlack, Canoville &
300 Chinsamy, 2012; Ray, Botha-Brink & Chinsamy-Turan, 2012). All authors agree on the fact that
301 dicynodonts share primary bone tissue that consists of mainly fibrolamellar bone with a
302 plexiform to laminar arrangement of vascular canals, suggesting overall fast rates of growth and
303 high metabolic demands. Uninterrupted fibrolamellar bone in early ontogenetic stages and
304 annuli, as well as LAGs only appearing during later stages of ontogeny (50 % of adult size),
305 characterise several dicynodont taxa (Ray & Chinsamy, 2004; Botha-Brink & Angielczyk 2010;
306 see also Ray, Botha-Brink & Chinsamy-Turan, 2012b). The occurrence of parallel-fibred bone in
307 the periphery of the cortex indicates a decrease in growth rate suggesting onset of reproductive
308 maturity (e.g. Castanet & Baez, 1991; Sander, 2000; Chinsamy-Turan, 2012). Peripheral rest
309 lines in a few genera suggest asymptotic growth (Green, Schweitzer & Lamm, 2010). For some
310 taxa it was possible to determine ontogenetic stages by bone histological features (Ray &
311 Chinsamy, 2004; Ray, Chinsamy & Bandyopadhyay, 2005; Ray, Bandyopadhyay & Appana,
312 2010). Most dicynodonts are characterised by a thick bone cortex independent of body size
313 suggesting a fossorial life style or digging habits (Botha-Brink & Angielczyk, 2010), whereas the
314 life style of some taxa remains unclear (Germain & Laurin, 2005; Ray, Bandyopadhyay &
315 Appana, 2010; Nasterlack, Canoville & Chinsamy, 2012).
316 *Gorgonopsia and Therocephalia* – Compared to other non-mammalian synapsids, sampling of
317 the Middle to Late Permian carnivorous gorgonopsians and the Permotriassic therocephalians
318 has been more limited (Botha & Chinsamy, 2000; Botha & Chinsamy, 2004; Botha & Chinsamy,
319 2005; Ray, Botha & Chinsamy, 2004; Chinsamy & Abdala, 2008; Botha-Brink, Abdala &
320 Chinsamy, 2012; Sigurdsen et al., 2012; Chinsamy-Turan, 2012b; Huttenlocker & Botha-Brink,
321 2013; Huttenlocker & Botha-Brink 2014). The earliest contributions on gorgonopsian and

therocephalian bone histology were performed by Ricqlès (1969; 1975; 1978). He found fibrolamellar bone in two therocephalian species and in the long bones of five gorgonopsian taxa with partially thick compacta and mainly longitudinal vascularisation. The histological traits found suggested differential growth rates between a basal therocephalian from the Middle Permian of South Africa and a more derived Late Permian whaitsiid therocephalian. Because of comparatively higher vascularisation in the radius of the whaitsiid, Ricqlès (1969) suggested that therocephalians might have grown at higher rates later in their phylogeny. Recently, Huttenlocker and Botha-Brink (2014) performed a phylogenetic survey of limb bone histology in therocephalians from the Middle Permian through the Middle Triassic of the Karoo Basin, South Africa. They sampled eighty limb bones representing eleven genera of therocephalians using skeletal growth, including cortical vascularity and mean primary osteon diameters as histological indicators, and assessed for correlations with other biologically significant variables (e.g. size and robustness). Smaller-bodied descendants tended to have lower vascularity than their phylogenetically larger-bodied ancestors. Bone wall thickness tended to be high in early therocephalians and lower in gracile-limbed baurioid therocephalians. However, clade-level patterns deviated from previously studied within-lineage patterns (e.g. *Moschorhinus* displayed higher vascularity in the Triassic than in the Permian despite its smaller size). Therefore, Huttenlocker and Botha-Brink (2014) argued for a synergistic model of size reductions for Triassic therocephalians, influenced by within-lineage heterochronic shifts in survivor taxa and phylogenetically inferred survival of small-bodied taxa that had evolved short growth durations.

Non-mammalian cynodonts – Cynodonts represent the last major synapsid lineage to appear in earth history with mammals as living representatives (Fig. 2). Many articles have been published

345 on non-mammalian cynodont histology in recent years (e.g. Ricqlès, 1969; Botha & Chinsamy
346 2000; Botha & Chinsamy, 2004; Botha & Chinsamy, 2005; Ray, Botha & Chinsamy, 2004;
347 Chinsamy & Abdala, 2008; Botha-Brink, Abdala & Chinsamy, 2012; Chinsamy-Turan, 2012b).
348 Fibrolamellar bone is present to a varying degree in all cynodonts. Considerable variation in
349 vascular density and orientation and the presence/absence of growth marks such as LAGs are
350 evident. When observed within the phylogenetic context, there is an overall increase in bone
351 deposition rate. This is indicated by an increasing prevalence of highly vascularised fibrolamellar
352 bone in phylogenetic later cynodonts (Botha-Brink, Abdala & Chinsamy, 2012). Several factors
353 are discussed to influence the microstructure and therefore being responsible for the
354 aforementioned variability: phylogeny, biomechanics, ontogeny, body size, lifestyle preferences,
355 and environmental influences (Cubo et al., 2005; Kriloff et al., 2008; Botha-Brink, Abdala &
356 Chinsamy, 2012). Padian (2013) emphasises that the correlation between fibrolamellar bone and
357 high growth rates as well as endothermy is still valid, although fibrolamellar bone is known to
358 occur in rare cases in ectothermic reptiles such as crocodiles and turtles.
359 *Multituberculata and early mammals* – Studies on multituberculate (see Fig. 3 for mammalian
360 groups discussed below) and in general stem mammalian histology are scarce. Enlow & Brown
361 (1958) described the section of a mandible of *Ptilodus*. Its cortex consisted of lamellar bone with
362 a central region of indistinct and unorganised lamellae, in which lacunae and cell spaces as well
363 as radial vascular canals were present. Morphological studies have suggested different kinds of
364 locomotion within the group (saltatorial, fossorial, scansorial, and arboreal; Kielan-Jaworowska,
365 Zifelli & Luo, 2004), which might be reflected in the microstructure of the appendicular bones.
366 Chinsamy & Hurum (2006) analysed in a comparative study the bone tissue of long bones and
367 one rib of multituberculates and early mammals. They showed that *Morganucodon* and

multituberculates (*Kryptobataar*, *Nemegtbataar*) ~~ha~~ ~~been~~ characterised by fibrolamellar/woven-fibred bone at early stages of ontogeny and later on by parallel-fibred or lamellar bone. These finds pointed towards relatively h rates compared to the late Mesozoic eutherians *Zalambdalestes* and *Barunlestes* with periodic growth pauses as indicated by the occurrence of LAGs. Comparisons of morganucodontid and early mammalian bone microstructure with that of non-mammalian cynodonts, extant monotremes, and placentals indicated significant differences in the rate of osteogenesis in the various groups. The authors concluded multituberculates and Mesozoic eutherians to have had slower growth rates than modern monotremes and placentals and that the sustained, uninterrupted bone formation among multituberculates may have been an adaptive attribute prior to the K−Pg event, but that a flexible growth strategy implying periodic growth pauses of the early eutherians was more advantageous thereafter.

Monotremata – Monotremes are represented today by three genera (*Ornithorynchus*, *Tachyglossus*, and *Zaglossus*) of specialized skeletal morphology. Their poor fossil record includes material from Australia and South America (Pascual et al., 1992; Musser and Archer 1998). Accordingly, the histology of monotremes has been scarcely studied. Enlow and Brown (1958) were the first to describe sections of long bones and ribs of *Platypus* and *Echidna*. Chinsamy & Hurum (2006) described the femoral bone tissue of *Ornithorhynchus* as being a mixture of woven-fibred bone with lamellar bone deposits. Additionally, large parts of the compacta consisted of compacted coarse cancellous bone. The type of vascularisation and the orientation of the vascular channels varied from simple blood vessels with longitudinal, circular and radial orientations to primary osteons with longitudinal and reticular arrangements. Only isolated secondary osteons were present.

391 *Marsupialia* – Despite marsupials the second most diverse group of living mammals,
392 their bone histology is poorly studied so far. Early contributions are those of Enlow & Brown
393 (1958) and Singh (1974) on the marsupial *Didelphis*. Our study of new samples of the white-
394 eared opossum *Didelphis albiventris* and the latrine opossum *Lutreolina crassicaudata* (Table 1)
395 essentially confirms their observations.
396 The bone cortex of *Didelphis* long bones is characterised by a compacta surrounding the
397 medullary cavity. The bone matrix is dominated by parallel-fibered bone (Figs. 4A-C). Towards
398 the inner part, the amount of woven-fibered bone increases (Fig. 4C). In most specimens
399 remodelling is restricted to isolated secondary osteons as described by Enlow & Brown (1958).
400 In specimen PIMUZ A/V 5278, remodelling is abundant in the central part of the cortex, being
401 formed by Haversian bone with obliquely oriented and irregularly shaped secondary osteons.
402 Inner and outer circumferential layers are present. The inner circumferential layer consists of
403 lamellar bone. The outer circumferential layer is dominated by parallel-fibered bone. The
404 thickness of this layer varies between specimens. Except in one specimen showing one LAG, no
405 LAGs are present in the analysed specimens suggesting constant growth rates. The bone cortex is
406 well vascularised up to the outer part of the cortex (see also Enlow & Brown, 1958), with an
407 irregular pattern, i.e. radial, oblique, but mainly longitudinal primary vascular canals. *Lutreolina*
408 shows a primary bone matrix that is dominated by parallel-fibered bone with simple primary
409 longitudinal and radial to oblique vascular canals (Figs. 4D-F). Remodelled areas are
410 characterised by partially oblique secondary osteons (Fig. 4F). The inner circumferential layer is
411 thin and formed by lamellar bone. The outer circumferential layer is, if present, formed by
412 parallel-fibered bone. LAGs are not developed. The vascularity is less dense than in *Didelphis*.

413 The combination of parallel-fibered bone with low vascularisation suggests slow apposition rates
414 (Chinsamy-Turan, 2012b; Huttenlocker, Woodward & Hall, 2013).
415 *Xenarthra* – Early contributions on xenarthran bone histology are Quekett (1849; 1855) and
416 Enlow and Brown (1958). Because dermal armour is an outstanding feature of xenarthrans,
417 several studies focussed on the histology of osteoderms and dermal ossicles (e.g. Wolf, 2007;
418 Wolf, 2008; Chávez-Aponte et al., 2008; Hill, 2006; Vickaryous & Hall, 2006; Krmpotic et al.,
419 2009; Vickaryous & Sire, 2009; Wolf, Kalthoff & Sander, 2012; Da Costa Pereira et al., 2012).
420 These data shed light on soft tissue structures of extinct xenarthrans, their phylogenetic
421 relationships as well as their functional morphology, which otherwise are not available. The most
422 detailed study up to date dealing with xenarthran long bone histology was performed by Straehl
423 et al., 2013 (but see also Ricqlès, Taquet & Buffrénil, 2009). Straehl and colleagues sampled
424 sixty-seven long bones of nineteen genera and twenty-two xenarthran species and studied bone
425 microstructure as well as bone compactness trends. Primary bone tissue consists of a mixture of
426 woven, parallel-fibred and lamellar bone. Irregularly shaped vascular canals show longitudinal,
427 reticular or radial orientation. Anteaters are the only sampled taxa showing laminar orientation.
428 Armadillo long bones are characterised by obliquely oriented secondary osteons in transverse
429 sections, reflecting their complex morphology. LAGs are common in xenarthrans although being
430 restricted to the outermost part of the bone cortex in armadillo long bones. Moreover, cingulates
431 (armadillos and closely relative extinct taxa) show lower bone compactness than pilosans (sloths)
432 and an allometric relationship between humeral and femoral compactness. Straehl and colleagues
433 emphasise that remodelling is more developed in larger taxa as indicated by dense Haversian
434 bone in adult specimens and discuss increased loading as a possible cause. Amson et al. (2014)
435 assessed the timing of acquisition of osteosclerosis (increase in bone compactness) and

436 pachyostosis (increase in bone volume) in long bones and ribs of the aquatic sloth *Thalassocnus*
437 from the Neogene of Peru as the main osteohistological modifications of terrestrial tetrapods
438 returning to water. They showed that such modifications can occur during a short geological time
439 span, i.e. *ca* 4 Ma. Furthermore, the strongly remodelled nature of xenarthran bone histology
440 allowed the reassignment of a rib previously ascribed to a sirenian to the aquatic sloth (Amson et
441 al., 2015).

442 *Afrotheria* – Early contributions on the bone histology of afrotherians are Aeby (1878)
443 and Schaffer (1890) on sirenians and proboscideans, Nopcsa & Heidsieck (1934) on sirenians,
444 Vanderhoof (1937), Enlow & Brown (1958), Kaiser (1960), Mitchell (1963; 1964) on sirenians
445 and desmostylians, and Ezra & Cook (1959) as well as Cook, Brooks & Ezra-Cohn (1962) on
446 elephantids. Ricqlès & Buffrénil (1995) described pachyosteosclerosis in the sirenian
447 *Hydrodamalis gigas*. Buffrenil et al. (2008; 2010) studied the ribs of 15 extant and extinct
448 sirenian species representing 13 genera, one desmostylian, and 53 specimens of 42 extant species
449 of terrestrial, aquatic or amphibious mammals. Primary bone tissue in young specimens is
450 constituted by fibrolamellar bone, whereas with increasing age, parallel-fibred bone tissue with
451 longitudinal vascular canals and frequent LAGs is deposited. The authors showed that
452 pachyostosis is subsequently regressed during evolution of the clade. In contrast, only by the end
453 of the Eocene, osteosclerosis was fully developed. It was argued that variable degrees of
454 pachyostosis and osteosclerosis in extinct and extant sirenians were caused by similar
455 heterochronic mechanisms bearing on the timing of osteoblast activity. Hayashi et al. (2013)
456 analysed the histology of long bones, ribs, and vertebrae of four genera of desmostylians (usually
457 considered as tethytherians, but see Cooper et al., 2014) and 108 specimens of extant taxa (ribs:
458 19 taxa, humeri: 62 taxa, femora: 16 taxa, vertebrae: 11 taxa) with various phylogenetic positions

459 and ecologies by using thin sections and CT-scan data. Primary bone tissue in desmostylians
460 consisted of parallel-fibred bone with multiple LAGs. By comparisons with extant mammals,
461 they found that *Behemetops* and *Palaeoparadoxia* show osteosclerosis, *Ashoroa*
462 pachyosteosclerosis (i.e. a combination of increase in bone volume and compactness), while
463 *Desmostylus* shows an osteoporotic-like pattern (i.e. decrease in bone compactness) instead.
464 Since it is known from extant mammals that bone mass increase provides hydrostatic buoyancy
465 and body trim control suitable for passive swimmers and shallow divers, whereas spongy bones
466 are associated with hydrodynamic buoyancy control in active swimmers, they concluded that all
467 desmostylians achieved an essentially aquatic lifestyle. However, the basal taxa *Behemotops*,
468 *Paleoparadoxia* and *Ashoroa* could be interpreted as shallow water swimmers hovering slowly
469 or walking on the bottom, whereas the derived taxon *Desmostylus* was a more active swimmer.
470 The study has therefore shown that desmostylians are the second mammalian group after
471 cetaceans to show a shift from bone mass increase to decrease during their evolutionary history.
472 As several tethytherian taxa are aquatic, the question of the ancestral lifestyle of the clade
473 was raised. A femur and a humerus of the Eocene proboscidean *Numidotherium* were sampled
474 by Mahboubi et al. (2014). These authors recognised “large medullar cavities” (p. 506), which
475 was considered as suggestive of terrestrial habits. However, the illustrations provided by
476 Mahboubi et al. (2014) show no opened medullary cavity, as trabecular bone occupies most of
477 the cross-sectional area (labelled “medullary bone” by Mahboubi et al., 2014: Fig. 5).
478 Sander & Andrassy (2006) described the bone tissue of *Mammuthus primigenius* long
479 bones as laminar fibrolamellar bone. Due to poor preservation of the fossil bone tissue, the
480 authors have not been able to definitely confirm the occurrence of LAGs. The valuable study of
481 Curtin et al. (2012) dealt with two aspects of bone histology. First, they described for the first

time the bone tissue of fifteen bones (femora and tibiae) of eleven specimens of late-term-fetal, neonatal, and young juvenile extant and extinct elephantids representing four species, including the insular dwarf mammoth *Mammuthus exilis* from the Late Pleistocene of Santa Rosa Island of the Californian Channel Islands. The bone tissue they found was predominantly laminar fibrolamellar bone. Remarkable was a distinct change in tissue microstructure marking the boundary between prenatal and postnatal bone deposition, i.e. a higher amount of large longitudinal vascular canals suggesting slightly higher postnatal growth rates. Secondly, besides histological thin sections, Curtin and colleagues employed synchrotron microtomography (SR-µCT) for noninvasively obtaining high-resolution image-"slices". They showed that, in comparison to histological sectioning, the SR-µCT data lack shrinkage, distortion or loss of tissue, as is usually the case in histological sections. However, they stated that the quality of histological detail observable is by far superior in histological thin sections. The virtual microtomography enabled the authors to rank specimens by ontogenetic stage and quantified vascular patterns. They showed that bones of the Columbian mammoth, *M. columbi* had the thickest and largest number of laminae, whereas the insular dwarf mammoth, *M. exilis*, was characterised by its variability in that regard. The authors concluded that, qualitatively, patterns of early bone growth in elephantids are similar to those of juveniles of other tetrapods, including dinosaurs.

Notoungulata – Notoungulates are an extinct, largely diverse, endemic group of Cenozoic South American mammals, ecologically similar to current hoofed ungulates. Only four taxa (*Toxodon*, *Nesodon*, *Mesotherium*, and *Paedotherium*) were subject to histological studies (Ricqlès, Taquet & Buffrénil, 2009; Forasiepi et al., 2014; Tomassini et al., 2014) from the more than 150 species recognised in the group. The bone samples were characterised by a well-vascularised compact

505 cortex with mostly longitudinal vascular canals. Few irregularly oriented canals could also be
506 found. Osteocyte lacunae were large and very abundant. Haversian bone was recorded in
507 *Toxodon*, *Nesodon*, and *Mesotherium*. This is a common feature in mammalian bone (Enlow &
508 Brown, 1958), probably caused by increased loading in large-bodied species as discussed by
509 Straehl et al. (2013) for xenarthrans. Areas of primary bone matrix were visible between
510 secondary osteons, which displayed a mostly parallel-fibered to lamellar organisation. Localized
511 areas of woven bone characterised by round osteocyte lacunae were also present. The most
512 external layer of the cortex consisted of parallel-fibred bone with only very few secondary
513 osteons and was in clear contrast to the heavily remodelled inner cortex. The study of Tomassini
514 et al. (2015) on the palaeohistology of hemimandibles of *Paedotherium bonaerense* from the
515 early Pliocene of Argentina discussed the processes affecting fossil remains before and after
516 burial.

517 *Pantodonta* - Pantodonts are an extinct group of mammals that comprised large-bodied,
518 heavily built omnivores and herbivores, from the Paleocene and Eocene of Laurasia. Only one
519 study (Enlow and Brown 1958) examined the bone histology of this group. The rib of the Eocene
520 pantodont *Coryphodon* showed primary lamellar bone with longitudinal vascularisation.

521 *Laurasiatheria – Eulipotyphla* - The comprehensive work of Enlow & Brown (1958)
522 gave the first contribution on eulipotyphlan bone histology. They described the primary bone
523 tissue of a *Talpa* tibia and a *Sorex* mandible as almost completely avascular lamellar bone. A
524 juvenile humerus and radius showed in their outer cortex a “disorganised” (Enlow & Brown,
525 (1958: p. 190) called it, being accompanied by oblique, radial, circumferential or longitudinal
526 simple vascular canals. Klevezal (1996) discussed eulipotyphlan histology by emphasising
527 growth marks (LAGs) in the bone cortex of mandibles and their value for skeletochronology.

Meier et al. (2013) studied the bone compactness of humeri of eleven extant and eight fossil talpid species and two non-talpid species. They could not detect any pattern of global compactness related to biomechanical specialization, phylogeny or size and concluded that at this small size the overall morphology of the humerus plays a predominant role in absorbing load. Morris (1970) evaluated the applicability of LAGs in extant hedgehog mandibles and found high correlation between age and LAG count.

In the giant galericine "hedgehog" *Deinogalerix* from the palaeoisland of Gargano (Table 1), Italy, the bone tissue at the inner layer of femur RGM.178017 and humerus RGM.425360 is characterised by parallel-fibred bone, whereas the outer layer and the trabecular bone is built by lamellar bone (Figs. 5A-C). In the bone cortex, simple longitudinal vascular canals and primary osteons are present. Primary bone tissue is partially replaced by irregularly shaped partly oblique secondary osteons. In the femur corresponding to an adult individual, five LAGs can be distinguished (Fig. 5C) indicating an individual age of minimum five years.

Chiroptera – Enlow & Brown (1958) described the primary bone tissue in chiropterans as lamellar bone surrounding a non-cancellous medullary cavity. Klevezal (1996) described the presence of LAGs in chiropteran bone tissue. Herdina et al. (2010) described the bone tissue of the baculum of three *Plecotus* species as lamellar bone surrounding a small medullary cavity similar to the arrangement of a Haversian system whereas the ends of the bone consisted of woven-fibred bone.

Perissodactyla – Enlow & Brown (1958), Sander & Andrassy (2006), Cuijpers (2006), and Hillier & Bell (2007) described long bones and ribs of fossil and extant equids as being primarily plexiform fibrolamellar with longitudinal vascular canals, accompanied by extensive remodelling including the occurrence of dense Haversian bone. Zedda et al. (2008) found a high

amount of Haversian tissue in extant horses and cattle. Osteons of the horse were more numerous and composed of a higher number of well-defined lamellae when compared to those of cattle. Diameter, perimeter and area of osteons and Haversian canals were always higher in horses than in cattle and this pattern was related to their different locomotor behaviour. Enlow and Brown (1958) additionally described a stratified, circumferential pattern of vascular canals in a mandible of a Miocene chalicothere (*Moropus*), i.e. laminar fibrolamellar bone tissue *sensu* Francillion-Vieillot et al. (1990). The authors demonstrated an identical pattern of bone tissues and vascular canals in several ribs of fossil tapirs from the Eocene. Sander & Andrassy (2006) described bone tissue of tibiae of Late Pleistocene woolly rhinocerotid (*Coelodonta antiquitatis*). They found predominantly laminar fibrolamellar bone as primary bone type besides a high amount of Haversian bone. Ricqlès, Taquet & Buffrénil (2009) described thin sections of several extant and extinct perissodactyls including chalicotheres, describing the distribution of primary and secondary bone as well as vascularisation. Cooper et al. (2014) considered anthracobunids as stem-perissodactyls, and concluded osteosclerosis in limb bones and ribs of anthracobunids to be consistent with the occupation of shallow-water habitats.

A rib of the giant rhinocerotoid *Paraceratherium* sp. (Fig. 1G, Table 1) from the Miocene of Turkey displays dense Haversian bone (Fig. 1I), whereas the bone cortex is heavily recrystallized and does not allow observations on primary bone.

Cetartiodactyla – Enlow & Brown (1958) gave a comprehensive overview on the bone histology of artiodactyls. The Miocene artiodactyls *Merycoidodon* and *Leptomeryx* showed in mandibles, maxillas, and ribs a reticular pattern of primary vascularisation next to secondary Haversian tissue. Extant taxa showed essentially plexiform fibrolamellar bone in long bones and reticular bone tissue in skull bones and mandibles. Singh (1974) studied the long bone tissue of a

574 mature specimen of the blue duiker *Cephalophus manticola*, and two perinatal specimens of the
575 Indian sambar *Cervus unicolor* and the reindeer *Rangifer tarandus*. Whereas *Cephalophus*
576 showed primary longitudinal vascularisation, the perinatal cervids revealed a reticular pattern of
577 vascular canals. Plexiform fibrolamellar bone (Figs. 1B, 1C, 1E, 1F) was confirmed as primary
578 bone tissue in artiodactyls in subsequent publications (Klevezal 1996; Horner, Ricqlès & Padian,
579 1999; Cuijpers, 2006; Sander & Andrassy, 2006; Hillier et al., 2007; Köhler et al., 2012; Marin-
580 Moratalla, Jordana & Köhler, 2013; Kolb et al., 2015). Marin-Moratalla et al. (2014) identified
581 the primary bone tissue in bovids as laminar. They studied 51 femora representing 27 ruminant
582 species in order to determine the main intrinsic or extrinsic factors shaping the vascular and
583 cellular network of fibrolamellar bone. Thus, the authors examined the correlation of certain life
584 history traits in bovids, i.e. body mass at birth and adulthood as well as relative age at
585 reproductive maturity. Quantification of vascular orientation and vascular and cell densities
586 revealed that there is no correlation with broad climatic categories or life history. Instead, the
587 authors found correlation with body mass since larger bovids showed more circular canals and
588 lower cell densities than did smaller bovids. Mitchell and Sander (2014) suggested a three front
589 model consisting of an apposition front, a Haversian substitution front, and a resorption front,
590 and applied this model successfully to a humerus of red deer *Cervus elaphus*. They found
591 moderate apposition and remodelling as well as slow resorption in the red deer specimen.
592 Hofmann, Stein & Sander (2014) examined the lamina thickness in bone tissue (LD) in
593 sauropodomorph dinosaurs and 17 mammalian taxa, including artiodactyls and perissodactyls.
594 They found that LD is relatively constrained within the groups and that mean mammalian LD
595 differs significantly from mean sauropodomorph LD. LD in suids was higher than in other
596 mammals. The authors therefore concluded that laminar vascular architecture is most likely

597 determined by a combination of structural, functional as well as vascular supply and
598 physiological causes.

599 For the present study, the bone cortex of one small (CKS 110/B), one intermediate (CKS
600 122/B), and one large juvenile (subadult; CKS 117) of the extinct Pleistocene dwarf
601 hippopotamid of Cyprus, *Hippopotamus minor* (also called *Phanourios minor*, see van der Geer
602 et al., 2010) were examined (Table 1). In the juvenile femora the bone tissue is characterised by
603 reticular to plexiform fibrolamellar bone with an endosteal, inner circumferential layer consisting
604 of lamellar bone (Fig. 6). The bone is generally highly vascularised with primary longitudinal
605 vascular canals and primary osteons towards the outer part of the cortex. There are no Haversian
606 systems in the small juvenile (Fig. 6B), although their content increases during ontogeny and is
607 highest in the subadult specimen. Although heavily recrystallized, an adult tibia of
608 *Hippopotamus minor* shows strong remodelling with partially dense Haversian bone occurring
609 from the inner to the outermost part of the cortex. Towards the outer cortex of the subadult femur
610 (Fig. 6D) and typically for large mammals, the amount of parallel-fibred bone within the
611 fibrolamellar complex increases, indicating a decrease in growth rate.

612 Another taxon sampled for the current study is *Sinomegaceros yabei* (Table 1), which is,
613 as *Megaloceros*, a large-sized megacerine deer. Although a thorough description is prevented by
614 the suboptimal preservation of the specimens, some of their histological features can be given
615 here. The primary bone of the inner cortex is highly vascularised, being formed by fibrolamellar
616 tissue with a mostly plexiform vascularisation. The outer cortex is in turn weakly vascularised.
617 The adult femur OMNH QV-4062 features seven LAGs (Fig. 7), with a 2.57 mm thick second
618 growth zone, which is even greater than the extreme values found in the elk, *Alces* and
619 *Megaloceros* (Kolb et al., 2015), and which indicates, as in the latter taxa, a high growth rate.

Several authors focused on the bone histology of cetaceans and sirenians for their peculiar aquatic lifestyle. Enlow & Brown (1958) described the primary bone tissue of skull bones and vertebrae of the porpoise (*Phocoena phocoena*) as featuring a reticular vascularisation with a high amount of remodelling including the occurrence of dense Haversian bone. Buffrénil and colleagues studied the microstructure of baleen whale bone tissue in several works. They found annually deposited well-defined LAGs in mandibular bone tissue of the common porpoise, *Phocoena phocoena* (Buffrénil, 1982). The humeral bone tissue of the common dolphin (*Delphinus delphis*) shows a cancellous texture without a free medullary cavity and more bone being eroded than deposited during ontogeny indicating an osteoporotic-like process (Buffrénil & Schoevaert, 1988). Buffrénil & Casinos (1995), by using standard microscopic methods, and Zylberberg et al. (1998), by using scanning and transmission electron microscopy, studied the rostrum of the extant Blainville's beaked whale *Mesoplodon densirostris*, demonstrating a high density because of hypermineralised tissue with longitudinal fibres in dense Haversian bone. Buffrénil, Dabin & Zylberberg (2004) demonstrated that the petro-tympanic bone complex in common dolphins consists of reticular to laminar fibrolamellar bone, initially being deposited as loose spongiosa with hypermineralised tissue and without Haversian remodelling. Two Eocene archaeocete taxa were shown to feature pachyostosis with hyperostosis (excessive bone growth) of the periosteal cortex very similar to the condition present in some sirenians (Buffrénil et al., 1990). The comparative study of Gray et al. (2007) analysed the ribs of ten specimens representing five extinct cetacean families from the Eocene as they make their transition from a terrestrial/semiaquatic to an obligate aquatic lifestyle over a 10-million-year period. The authors compared those data to nine genera of extant mammals, amongst them modern dolphins, and found profound changes of microstructure involving a shift in bone function. The mechanisms of

643 osteogenesis were flexible enough to accommodate the shift from a typical terrestrial form to
644 osteosclerosis and pachyosteosclerosis, and then to osteoporosis in the first quarter of the
645 evolutionary history of cetaceans. The limb bones and ribs of *Indohyus*, a taxon closely related to
646 cetaceans, were shown to feature osteosclerosis, and considered as indicative of the use of
647 bottom-walking as swimming mode (Thewissen et al., 2007; Cooper et al., 2012). Ricqlès,
648 Taquet & Buffrénil (2009) published the description of a rediscovered collection of thin sections
649 from the 19th century French palaeontologist Paul Gervais including sections of cetaceans. The
650 most recent study on the bone microstructure of cetaceans is the one of Houssaye, Muizon &
651 Gingerich (2015) analysing the bone microstructure of ribs and vertebrae of 15 archaeocete
652 specimens, i.e. Remingtonocetidae, Protocetidae, and Basilosauridae using microtomography
653 and virtual thin-sectioning (i.e. CT scanning). They found bone mass increase in ribs and femora,
654 whereas vertebrae are essentially spongeous. Humeri changed from compact to spongeous
655 whereas femora in basilosaurids became, for not being involved in locomotion, reduced,
656 displaying strong osteosclerosis. The authors concluded that Remingtonocetidae and
657 Protocetidae were probably shallow water swimmers, whereas basilosaurids, for their osseous
658 specializations similar to those of modern cetaceans, are considered more active open-sea
659 swimmers.

660 *Creodonta* – As it is the case for many other vertebrate taxa, Enlow and Brown (1958)
661 are until today the only workers to have analysed the bone tissue of mammalian predators from
662 the Paleogene and Early Neogene of North America, Africa, and Eurasia, the “creodonts”. Bone
663 tissue of mandibles, ribs, and long bones has shown to consist of primary lamellar bone with
664 longitudinal/radial vascularisation and secondary Haversian tissue, in general similar to the bone
665 tissue found in modern carnivorans.

Carnivora – Enlow & Brown (1958) studied the mandible bone tissue of *Ursus* and found primary reticular bone and secondary dense Haversian bone, whereas a rib showed only dense Haversian bone. In the outer part, the bone cortex of *Ursus* consisted of plexiform bone. Chinsamy, Rich & Vickers-Rich (1998) found several LAGs in the zonal bone cortex of the polar bear. Hayashi et al. (2013) reported that the polar bear (*Urusus maritimus*) displays microanatomical features close to those of active swimmers in its limb bones, particularly in the humerus, and intermediate between aquatic and terrestrial taxa in the femur, despite its morphological features, which do not show particular adaptation for swimming. However, *U. maritimus* long bones still displayed a true medullary cavity. The authors suggested that this result, and notably the apparently stronger adaptation of the humerus for an aquatic mode of life, is probably linked to its swimming style because *U. maritimus* uses the forelimbs as the main propulsors during swimming.

Mephitis (skunk), *Procyon* (raccoon), *Mustela* (badger), *Felis* (cat), *Canis* (dog), and *Urocyon* (fox) all possess reticular and radial primary bone (Enlow & Brown 1958). However, the bone cortex of adult specimens in these taxa was dominated by secondary Haversian bone. The outer cortex of *Canis* was composed of primary plexiform bone tissue. The mongoose (*Herpestes*) showed in its femur primary longitudinal vascularised bone devoid of Haversian remodelling whereas the bone cortex of the American mink (*Neovison vison*) was composed of reticular and Haversian bone.

Singh (1974) found in felids and mustelids lamellar bone with radial to longitudinal vascularisation. Klevezal & Kleinenberg (1969) found annual LAGs in the bone cortex of carnivores. Several works dealt with the accuracy of LAGs in carnivores in comparison to dental histology as a tool of age determination: Johnston & Beauregard (1969) (*Vulpes*), Pascale &

689 Delattre (1981) (*Mustela*), King (1991) (*Mustela*), Klevezal (1996) (*Mustela*, *Martes*), Pascal &
690 Castanet (1978) (*Felis*). The outcome was always in favour of dental cementum analysis.
691 Buffrénil & Pascal (1984) concluded that in mink mandibles the deposition of LAGs is not
692 strictly annual by using fluorescein and alizarin labelling.
693 The long bones of *Valenictus*, a Pliocene walrus (Odobenidae), were described as being
694 osteosclerotic (Deméré, 1994).
695 *Euarchontoglires – Rodentia* – Early contributions on rodent bone histology were made
696 by Enlow & Brown (1958) as well as Singh (1974). More recent ones are those of Klevezal
697 (1996) on rest lines and age determination, Martiniakova et al. (2005) on rat bone histology, and
698 Garcia-Martinez et al. (2011) on the bone histology of dormice. The bone tissue of rodents
699 mainly consists of lamellar or parallel-fibred bone with longitudinal vascularisation as primary
700 bone tissue. Development of Haversian bone is rare. Geiger et al. (2013) studied the bone cortex
701 of a femur of the giant caviomorph *Phoberomys pattersoni* from the Miocene of Trinidad, and
702 found it to be composed of lamellar-zonal bone. The specimen sampled showed alternating
703 layers of compacted coarse cancellous bone and parallel-fibered primary bone with a reticulum-
704 like structure. The authors reported Haversian tissue to be absent.
705 The femoral bone cortex of *Mikrotia magna*, a giant insular murine rodent from the Late
706 Miocene former island of Gargano (Italy; Table 1), consists merely of compact bone. The bone
707 matrix of the central part of the cortex is dominated by parallel-fibred bone with reticular
708 vascularisation being pervaded by irregularly shaped and partially obliquely oriented secondary
709 osteons (Figs. 8A-C), producing a distinct disorganised pattern (Enlow & Brown, 1958). The
710 inner and outer parts of the cortex are formed by lamellar bone with poor longitudinal but mainly
711 radial vascularisation. The thickness of those parts varies throughout the circumference of the

712 bone cortex and between samples. All the samples display LAGs. In the adult femur
713 RGM.792085, four to five LAGs are counted. Resorption cavities are present close to the
714 medullary cavity.

715 Thin sections of the femur of the dormouse *Leithia* sp. from the Pleistocene of Sicily
716 (Table 1) are characterised by a compact cortex. The primary bone matrix is formed by lamellar
717 bone pervaded by scarce and irregularly shaped and partially obliquely oriented secondary
718 osteons (Figs. 8D-F). There is no LAG, suggesting a constant apposition rate. Large resorption
719 cavities occur. The primary vascularisation is weak and limited to only few longitudinal to radial
720 vascular canals.

721 *Lagomorpha* – For this study four different species of ochotonids (*Prolagus*) were
722 investigated (Table 1). One mainland form (*Prolagus oeningensis* from La Grive France) and
723 three island forms: The giant species *Prolagus sardus* (Sardinia, Italy) (Fig. 9A) and *P.*
724 *imperialis* along with *P. apricenicus*, both from Gargano, Italy. Generally, the bone cortex of the
725 femur and the humerus of *Prolagus* is compact. It is characterised by a bone matrix changing
726 from parallel-fibered into lamellar bone from the central cortex towards the OCL (Figs. 9B-F).
727 An endosteal lamellar layer is present. In most specimens the parallel-fibred bone is partly
728 pervaded by irregularly shaped partially obliquely oriented secondary osteons, producing the
729 "subendosteal layer of Haversian-like bone" *sensu* Pazzaglia et al. (2015: Fig. 6B). The primary
730 bone cortex is in general weakly vascularised. Within the primary parallel-fibred bone, primary
731 and simple longitudinal vascular canals as well as radial and reticular vascular canals occur and
732 are arranged in an irregular manner. LAGs indicating minimum ages are present in some adult
733 specimens. *Prolagus oeningensis* (Figs. 9B, 9C) gives a maximum count of three LAGs,
734 *Prolagus apricenicus* a maximum count of two LAGs, and *Prolagus imperialis* as well as

735 *Prolagus sardus* each gives a maximum count of five LAGs (Figs. 9D-F). The femur of the
736 juvenile *Prolagus sardus* (NMB Ty. 4974) is in the inner part of the cortex characterised by
737 reticular vascularised fibrolamellar complex with a high amount of woven bone. Towards the
738 bone surface, the amount of parallel-fibered bone is increasing and the vascularisation changes
739 into longitudinal simple and primary vascular canals. In the area of the strongest curvature of the
740 cortex, primary bone tissue is pervaded by obliquely oriented irregularly shaped secondary
741 osteons. Our observations on lagomorph bone histology agree with Enlow and Brown's (1958)
742 observations on *Lepus*. The same is the case for the study of Pazzaglia et al. (2015), who studied
743 rabbit (*Oryctolagus cuniculus*) femora of different ontogenetic stages via micro CT-scanning.
744 However, what they call laminar respectively plexiform bone tissue is not in agreement with the
745 nomenclature of Francillon-Vieillot et al. (1990) used by us, i.e. longitudinal, radial, and reticular
746 vascularisation.
747 *Primates* - Again, Enlow & Brown (1958) were the first to describe the bone tissue of extinct
748 primates by sampling a mandible of the fossil Paleocene *Plesiolestes* and long bones of modern
749 primates. The authors described primary bone tissue formed by lamellar bone. Vascularisation
750 was mainly characterised by longitudinal primary vascular canals. Remodelling was partially
751 abundant and the organisation of Haversian bone was in some areas of the bone cortex even
752 dense. Those observations have been confirmed by the comparative studies of Cuijpers (2006)
753 and Hillier & Bell (2007) as well as the conceptual ones of Bromage et al. (2009; see also above)
754 and Castanet (2006; see also above). Castanet et al. (2004; see also above) found the inner and
755 thicker part of the bone cortex of *Microcebus* long bones to be formed by parallel-fibred bone
756 containing primary blood vessels and scarce primary osteons. In contrast, the outer part of the
757 cortex is not vascularised. Crowder & Stout (2012) have compiled a book regarding the current

758 utilisation of histological analysis of bones and teeth within the field of anthropology, including
759 the biology and growth of bone, histomorphological analysis, and age determination. There is
760 extensive literature on hominoids, especially on bone pathologies in *Homo sapiens*, and in order
761 not to go beyond the scope of this work, we cite here only some examples of publications in this
762 area. Martinez-Maza, Rosas & García-Vargas (2006) and Martinez-Maza et al. (2011) analysed
763 bone surfaces under the reflected light and scanning electron microscope in order to decipher
764 modelling and remodelling patterns in extant hominine facial skeletons and mandibles as well as
765 in Neanderthal mandibles, explaining specific morphological traits. Schultz and Schmidt-Schultz
766 (2014) examined fossil human bone and reviewed the methods and techniques of light
767 microscopy, scanning electron microscopy, and advantages of polarisation microscopy for
768 palaeoanthropology. In this context it is noteworthy that estimation of individual age in
769 anthropology is carried out by mainly two methods (Schultz & Schmidt-Schultz, 2014): (1) the
770 histomorphometric method (HMM) and (2) the histomorphologic method (HML). The HMM
771 method is applied mainly to long bones (e.g. Kerley, 1965; Drusini, 1987) and is based upon the
772 frequencies of osteons (Haversian systems), fragmented osteons (interstitial lamellae), non-
773 Haversian canals, and the percentage of the external circumferential lamellae. The HML method
774 is based upon the morphology (presence, size, shape, development) of external and internal
775 circumferential lamellae, osteons, fragmented osteons, and non-Haversian canals (e.g. Schultz,
776 1997). Skinner et al. (2015) studied pattern of trabeculae distribution of metacarpals in
777 *Australopithecus africanus* and Pleistocene hominins. They found a ‘human-like’ pattern,
778 considered as consistent with tool use. Ryan & Shaw (2015) quantified the proximal femur
779 trabecular bone structure using micro-CT data from 31 extant primate taxa (229 individuals) and
780 four distinct archaeological human populations (59 individuals) representing sedentary

781 agriculturalists and mobile foragers. Trabecular bone variables indicate that the forager
782 populations had significantly higher bone volume fraction, thicker trabeculae, and lower relative
783 bone surface area compared with the two agriculturalist groups. The authors did not find any
784 significant differences between agriculturalist and forager populations for trabecular spacing,
785 number, or degree of anisotropy. Ryan & Shaw concluded in revealing a correspondence
786 between human behaviour and bone structure in the proximal femur, indicating that more highly
787 mobile human populations have trabecular bone structure similar to what would be expected for
788 wild non-human primates of the same body mass, thus emphasising the importance of physical
789 activity and exercise for bone health and the attenuation of age-related bone loss.
790
791 **Selected contributions on mammalian histology**
792 In the following part, selected contributions on mammalian histology are separately
793 discussed, since they deserve a more detailed evaluation in our view because they address special
794 aspects and/or applications of palaeohistological work. Enlow's & Brown's (1958) outstanding
795 comparative work on mammalian bone histology is not further mentioned in this section, since it
796 is repeatedly discussed above.
797 Klevezal & Kleinenberg (1969) were the first to recognise the presence and importance
798 of rest lines in the bone cortex of mammals for skeletochronological studies (see also Chinsamy-
799 Turan, 2005). In their work, which was originally published in Russian in 1967, they found that
800 in mammals, unlike the zonal bone forming in reptiles, the recording part including LAGs is the
801 outer or periosteal zone (see also above). Klevezal (1996) found that not in every mammalian
802 taxon rest lines are formed from the first year of life. Therefore she suggested a variable
803 correction factor for different mammalian taxa, and concluded that the best structures for

804 recording growth and age are dentine and especially cementum (Klevezal, 1996). In her detailed
805 and comprehensive study of recording structures in mammals, she found that the growth rate of a
806 particular structure can change according to the growth rate of the whole organism and that
807 seasonal changes of growth intensity of an animal as a whole determine the formation of growth
808 layers. Klevezal (1996) argued that changes in humidity, not temperature, may play a role as
809 seasonal factor in growth.

810 Dumont et al. (2013) documented the microstructure of vertebral centra using 2D
811 histomorphometric analyses of vertebral centra of 98 therian mammal species that cover the
812 main size ranges and locomotor adaptations known in therian taxa. The authors extracted eleven
813 variables relative to the development and geometry of trabecular networks from CT scan mid-
814 sagittal sections. Random taxon reshuffling and squared change parsimony indicated a
815 phylogenetic signal in most of the variables. Furthermore, based on those variables, it was
816 possible to discriminate three categories of locomotion among the sampled taxa: a) terrestrial +
817 flying + digging + amphibious forms, b) coastal oscillatory aquatic taxa, and c) pelagic
818 oscillatory aquatic forms represented by oceanic cetaceans. Dumont and colleagues concluded
819 that, when specific size increases, the length of trabecular networks, as well as trabecular
820 proliferation, increase with positive allometry. They found that, by using six structural variables,
821 locomotion mode can be predicted with a 97.4% success rate for terrestrial forms, 66.7% for
822 coastal oscillatory, and 81.3% for pelagic oscillatory.

823 Sander & Andrassy (2006) described the occurrence of LAGs in 21 long bones (mainly
824 tibiae and metatarsals) of herbivorous mammals from the Late Pleistocene of Germany
825 comprising the extinct giant deer *Megaloceros giganteus*, the red deer *Cervus elaphus*, the
826 reindeer *Rangifer tarandus*, the extinct bovids *Bos primigenius* and *Bison priscus*, the equid

827 *Equus* sp., the extinct rhinocerotid *Coelodonta antiquitatis*, and the extinct elephantid
828 *Mammuthus primigenius*. All samples showed fibrolamellar bone and a varying degree of
829 remodelling and most of the long bones displayed LAGs. Because of the frequent find of LAGs
830 in endothermic animals the authors questioned the argument that LAGs in dinosaur bone indicate
831 ectothermy.

832 Köhler & Moyà-Solà (2009) examined the long-bone histology of *Myotragus*, a Plio-
833 Pleistocene bovid from the Balearic Islands. It revealed lamellar-zonal tissue throughout the
834 cortex, a trait exclusive to ectothermic reptiles. According to Köhler and colleagues, *Myotragus*
835 grew unlike any other mammal but similar to crocodiles at slow and flexible rates, ceased growth
836 periodically, and attained somatic maturity late by 12 years. The authors concluded that this
837 developmental pattern indicates that *Myotragus*, much like extant reptiles, synchronized its
838 metabolic requirements with fluctuating resource levels.

839 Kolb et al. (2015) performed a histological analysis of long bones and teeth representing
840 eleven extinct and extant cervid taxa, amongst them the dwarf island morphotypes of
841 *Candiacervus* from the Late Pleistocene of Crete and the giant deer *Megaloceros giganteus*, both
842 in a clade together with fallow deer (*Dama dama*) among extant species. Bone tissue types
843 observed have been similar, indicating a comparable mode of growth across the eight species
844 examined, with long bones mainly possessing primary plexiform fibrolamellar bone (Figs. 1B,
845 1C, 1E, 1F). Dwarf *Candiacervus* have been characterised by low growth rates, *Megaloceros* by
846 high rates, and the lowest recorded rates were those of the Miocene small stem cervid
847 *Procervulus praelucidus*. It can be noted that *Sinomegaceros yabei*, sampled for the present
848 study, features a very thick second growth zone, which suggests a high growth rate, comparable
849 to that of the closely related *Megaloceros*. Skeletal maturity estimates (see also above) indicated

late attainment in sampled *Candiacervus* and *Procervulus*. Tooth cementum analysis of first molars of two senile *Megaloceros giganteus* specimens revealed ages of 16 and 19 years whereas two old dwarf *Candiacervus* specimens gave ages of 12 and 18 years. Kolb et al. (2015) concluded that the bone histological condition found in *Candiacervus* has features in common with that of *Myotragus* (Köhler & Moyà-Solà, 2009), but is achieved with a lesser modification of bone tissue and suggested various modes of life history and size evolution among island mammals.

Discussion and conclusions

A large variety of bone tissues and vascularisation patterns is encountered in mammalian bone reaching from lamellar or parallel-fibred to fibrolamellar or woven-fibred bone, highly depending on taxon and individual age. A plexiform to laminar organisation of vascular canals within fibrolamellar bone is typically found in taxa containing large-bodied species such as non-mammalian synapsids, laurasiatherians, and afrotherians. The deposition of Haversian systems throughout ontogeny of synapsids is common, only in rodents their content is usually low. Table 2 gives a summary on general patterns of bone histological features encountered in major synapsid clades.

Histology of island mammals – Three juvenile specimens of the dwarf island hippopotamid *Hippopotamus minor* from the Late Pleistocene of Cyprus show reticular to plexiform fibrolamellar bone, which does not indicate an island-specific pattern of bone growth or life history but a mode of growth similar to continental hippopotamid relatives instead. The bone cortex of the dormouse *Leithia* sp. from the Pleistocene of Sicily is characterised by lamellar bone and low vascularisation. *Mikrotia magna*, the giant island rodent from the Late

873 Miocene of Gargano, Italy shows in the central part of the cortex parallel-fibred bone with
874 reticular vascularisation being pervaded by irregularly shaped and partially obliquely oriented
875 secondary osteons, whereas the inner and outer parts of the cortex are formed by lamellar bone.
876 Three fossil species of insular giant *Prolagus* and the fossil continental lagomorph *Prolagus*
877 *oeningensis* exhibit in their bone cortex mainly parallel-fibred bone and reticular, radial as well
878 as longitudinal vascularisation thus indicating similarity of bone histological arrangements in
879 continental and island species of rodents and lagomorphs. The highest minimum age found in
880 *Prolagus sardus* and *P. imperialis* of five years are well within the known longevities of extant
881 ochotonids such as *Ochotona princeps* (seven years in captivity) and *O. hyperborean* (9.4 years
882 in captivity) (Tacutu et al., 2013). A minimal individual age deduced from growth marks in the
883 bone tissue of *Deinogalerix* specimen RGM 178017 lies also well within the known longevities
884 for extant erinaceids such as *Erinaceus europaeus* (11.7 years in captivity), *E. concolor* (seven
885 years in captivity), and *E. amurensis* (9.4 years in captivity) whereas longevity data for extant
886 galericines are not yet available (Tacutu et al., 2013).

887 The insular bovid *Myotragus* dwelt on Majora for 5.2 Ma (Köhler & Moyà-Solà, 2009)
888 and therefore likely much longer than the insular forms examined in this study (van der Geer et
889 al., 2010). A high degree of bone histological and life history modification as described by
890 Köhler & Moyà-Solà (2009) for *Myotragus* in comparison to continental artiodactyls could not
891 be confirmed for the insular species of this study. The absence of modification of bone tissue and
892 longevity in insular lagomorphs, rodents, insectivores, and hippopotamids could be related to
893 shorter persistence times and different island size (Lomolino et al., 2012; Lomolino et al., 2013;
894 Kolb et al., 2015)., in line with Austad & Fischer (1991), McNab (1994; 2002; 2010), Raia,

895 Barbera & Conte (2003), Curtin et al. (2012), and Kolb et al. (2015). We therefore suggest the
896 presence of various modes of mammalian life history evolution on islands.
897
898 **Future research fields**
899 *New technologies* - 3D reconstructions attained by virtual image analysis gain increasing
900 importance for palaeontological research at the anatomical, microanatomical, and even
901 histological levels (Sanchez et al., 2012; Clément & Geffard-Kuriyama, 2010; Curtin et al.,
902 2012; see also Ricqlès, 2011). The potential advantages of virtual imaging as a method are
903 obvious: First, specimens do not have to be damaged for invasive sampling. Second, a third
904 dimension, usually gained by time consuming serial sectioning or preparation of orthogonally
905 oriented thin sections, is easily available. Third, virtual imaging techniques allow continuous
906 "zooming" from the histological to the micro- and macronatomical levels of structural
907 organisation. High resolution synchrotron virtual histology provides new 3D insights into the
908 submicron-scale histology of fossil and extant bones. This is based on the development of new
909 data acquisition strategies, pink-beam configurations, and improved processing tools (Sanchez et
910 al., 2012). Nevertheless, for the high resolution optical properties of a polarisation microscope
911 and their applications for identification and analysis of bone microstructure and as well for the
912 comparatively low amount of financial resources needed, traditional thin sections are far from
913 being completely replaced by virtual imaging techniques. Moreover, new statistical methods
914 allow extraction of phylogenetic signals from bone microstructure and of high specimen numbers
915 (Laurin, 2004; Laurin, Girondot & Loth, 2004; Cubo et al., 2008). High performance computers
916 additionally sustain attainment of ecological, biomechanical, and phylogenetic signals (Cubo et
917 al., 2005; Cubo et al., 2008; Laurin, Girondot & Loth, 2004; Laurin et al., 2004; Ricqlès & Cubo,

2010; Hayashi et al., 2013) taking into account the variability of bone tissues produced by multiple factors. The creation of histological databases will soon be necessary due to an increasing number of palaeohistological publications and growing collections of thin sections (Ricqlès, Castanet & Francillon-Vieillot, 2004; Ricqlès, Taquet & Buffrénil, 2009; Bromage, 2006; Kriloff et al., 2008; Scheyer, 2009-2015; Canoville & Laurin, 2010; O'Leary & Kaufmann, 2012).

Extant vertebrate biology - Actualistic models are essential for the interpretation of fossil hard tissues in every sense, no matter if developmental and life historical, histophysiological, morphological, ecological, or systematic. Living animals present the basis for inferring palaeobiological conclusions and this has already been done in several bone histological works (e.g. Canoville & Laurin, 2010; Köhler et al., 2012, Marin-Moratalla, Jordana & Köhler, 2013; Marin-Moratalla et al., 2014; Kolb et al. 2015).

Especially in regard of deciphering life history signals, the actualistic approach is and will become increasingly fundamental (e.g. Köhler & Moyà-Solà, 2009; Köhler et al., 2012; Marin-Moratalla, Jordana & Köhler, 2013; Marin-Moratalla et al., 2014; Kolb et al., 2015). Life history variables such as annual growth rate, somatic/sexual maturity, and longevity and their signal in bone microstructure help to understand the palaeobiology not only of fossil mammals but tetrapods in general. It is possible using bone histology to quantify growth rates and vascularisation or cellular density in mammals as a relative proxy for growth rate (Curtin et al., 2012; Kolb et al., 2015; Marin-Moratalla, Jordana & Köhler, 2013), whereby the existing literature on the paleobiology of dinosaurs has been used as a starting point. However, not every methodological approach used for dinosaurs is applicable or relevant for mammals (e.g.

941 Erickson, Curry Rogers & Yerby, 2001; Griebeler, Klein & Sander, 2013; Kolb et al., 2015). No
942 one stated it better than Armand de Ricqlès: „The possibilities of using bone histology of extant
943 vertebrates for various fundamental or applied research, whether on life history traits, ecology, or
944 microevolution, are simply boundless.“ (Ricqlès, 2011).
945

946 **Acknowledgments**

947 We thank Naturalis Biodiversity Center, Leiden, the Netherlands, Loïc Costeur
948 (Naturhistorisches Museum Basel, Switzerland), George Lyras (Museum of Paleontology and
949 Geology, University of Athens, Greece), Nigel Monaghan (National Museum of Ireland, Natural
950 History), Hiroyuki Taruno (Osaka Museum of Natural History, Japan), Frank Zachos and
951 Alexander Bibl (Naturhistorisches Museum Wien, Austria), Pierre-Olivier Antoine (Institut des
952 Sciences de l'Evolution-Montpellier, France), and Ebru Albayrak, (MTA Natural History
953 Museum, The General Directorate of Mineral Research and Exploration, Ankara, Turkey) for
954 organising and/or providing specimens for histological study. Alexandra Wegmann and Fiona
955 Straehl are thanked for help with bone histological preparation, and Madeleine Geiger for fruitful
956 discussions (all Palaeontological Institute of the University of Zurich, Switzerland).
957

958 **References**

959 Aeby C. 1878. Das histologische Verhalten fossilen Knochen- und Zahngewebes. *Archiv für*
960 *Mikroskopische Anatomie* 15:371-382.

961 Agustí J, and Antón M. 2002. *Mammoths, sabertooths and hominids*. New York: Columbia
962 University Press.

963 Amprino R. 1947. La structure du tissu osseux envisagee comme l'expression de différences dans
964 la vitesse de l'accroissement. *Archives de Biologie* 58:315-330.

965 Amson E, Muizon C de, Laurin M, Argot C, and Buffrénil V de. 2014. Gradual adaptation of
966 bone structure to aquatic lifestyle in extinct sloths from Peru. *Proceedings of the Royal Society*
967 *B* 281:1-6.

968 Amson E, Muizon C de, Domning DP, Argot C, and Buffrénil V de. 2015. Bone histology as a
969 clue for resolving the puzzle of a dugong rib in the Pisco Formation, Peru. *Journal of Vertebrate*
970 *Paleontology*: e922981.

971 Austad SN, and Fischer KE. 1991. Mammalian aging, metabolism, and ecology: Evidence from
972 the bats and marsupials. *Journal of Gerontology* 46:B47-53.

973 Bennett AF, and Ruben AJ. 1986. The metabolic and thermoregulatory status of therapsids. In:
974 Hotton N, MacLean PD, Roth JJ, and Roth EC, eds. *The ecology and biology of mammal-like*
975 *reptils*. Washington: Smithsonian Institution Press, 207-218.

976 Benson RBJ. 2012. The global interrelationships of basal synapsids: cranial and postcranial
977 morphological partitions suggest different topologies. *Journal of Systematic*
978 *Palaeontology* 10:601-624.

979 Boef M de, and Larsson HCE. 2007. Bone microstructure: quantifying bone vascular
980 orientation. *Canadian Journal of Zoology* 85:63-70.

981 Botha J, and Chinsamy A. 2000. Growth patterns deduced from the bone histology of the
982 cynodonts *Diademodon* and *Cynognathus*. *Journal of Vertebrate Paleontology* 20:705-711.

983 Botha J, and Chinsamy A. 2004. Growth and life habits of the Triassic cynodont *Trirachodon*,
984 inferred from bone histology. *Acta Palaeontologica Polonica* 49:619-627.

985 Botha J, and Chinsamy A. 2005. Growth patterns of *Thrinaxodon liorhinus*, a non-mammalian
986 cynodont from the Lower Triassic of South Africa. *Palaeontology* 48:385-394.

987 Botha-Brink J, Abdala F, and Chinsamy A. 2012. The radiation and osteohistology of
988 nonmammaliaform cynodonts. In: Chinsamy-Turan A, ed. *Forerunners of mammals: radiation,*
989 *histology, biology*. Bloomington: Indiana University Press, 223-246.

990 Botha-Brink J, and Angielczyk KD. 2010. Do extraordinarily high growth rates in Permo-
991 Triassic dicynodonts (Therapsida, Anomodontia) explain their success before and after the end-
992 Permian extinction? *Zoological Journal of the Linnean Society* 160:341-365.

993 Brink KS, and Reisz RR. 2014. Hidden dental diversity in the oldest terrestrial apex predator
994 *Dimetrodon*. *Nature Communications* 5:3269.

995 Bromage TG. 2006. Donald H. Enlow Digital Image Library. *Available at*
996 *http://www.nyu.edu/dental/enlow/* (accessed 13 May 2015).

997 Bromage TG, Lacruz RS, Hogg R, Goldman HM, McFarlin SC, Warshaw J, Dirks W, Perez-
998 Ochoa A, Smolyar I, Enlow DH, and Boyde A. 2009. Lamellar bone is an incremental tissue
999 reconciling enamel rhythms, body size, and organismal life history. *Calcified Tissue*
1000 *International* 84:388-404.

1001 Buffrénil V de. 1982. Données préliminaires sur la présence de lignes d'arret de croissance
1002 périostiques dans la mandibule du marsouin commun, *Phocoena phocoena* (L.), et leur
1003 utilisation comme indicateur de I'age. *Canadian Journal of Zoology* 60:2557-2567.

1004 Buffrénil V de, Astibia H, Pereda Suberbiola X, and Berreteaga A. 2008. Variation in bone
1005 histology of middle Eocene sirenians from western Europe. *Geodiversitas* 30:425-432.

1006 Buffrénil V de, Canoville A, D'Anastasio R, and Domning DP. 2010. Evolution of sirenian
1007 pachyosteosclerosis, a model-case for the study of bone structure in aquatic tetrapods. *Journal of*
1008 *Mammalian Evolution* 17:101–120.

1009 Buffrénil V de, and Casinos A. 1995. Observations histologiques sur le rostre de *Mesoplodon*
1010 *densirostris* (Mammalia, Cetacea, Ziphiidae): le tissu osseux le plus dense connu. *Annales des*
1011 *Sciences Naturelles, Zoologie, Paris, 13e Série* 16:21-36.

1012 Buffrénil V de, and Castanet J. 2000. Reptiles age estimation by skeletochronology in the Nile
1013 Monitor (*Varanus niloticus*), a highly exploited species. *Journal of Herpetology* 34:414-424.

1014 Buffrénil V de, Dabin W, and Zylberberg L. 2004. Histology and growth of the cetacean petro-
1015 tympanic bone complex. *Journal of Zoology* 262:371-381.

1016 Buffrénil V de, and Pascal B. 1984. Croissance et morphogenèse postnatales de la mandibule du
1017 vison (*Mustela vison*, Schreiber): données sur la dynamique et l'interprétation fonctionnelle des
1018 dépots osseux mandibulaires. *Canadian Journal of Zoology* 62:2026-2037.

1019 Buffrénil V de, Ricqlès Ad, Ray CE, and Domning DP. 1990. Bone histology of the ribs of the
1020 archaeocetes (Mammalia: Cetacea). *Journal of Vertebrate Paleontology* 10:455-466.

1021 Buffrénil V de, and Schoevaert D. 1988. On how the periosteal bone of the delphinid humerus
1022 becomes cancellous: ontogeny of a histological specialization. *Journal of Morphology* 198:149-
1023 164.

1024 Bybee PJ, Lee AH, and Lamm ET. 2006. Sizing the Jurassic theropod dinosaur *Allosaurus*:
1025 assessing growth strategy and evolution of ontogenetic scaling of limbs. *Journal of*
1026 *Morphology* 267:347-359.

1027 Canoville A, and Laurin M. 2010. Evolution of humeral microanatomy and lifestyle in amniotes,
1028 and some comments on palaeobiological inferences. *Biological Journal of the Linnean*
1029 *Society* 100:384-406.

1030 Castanet J. 1994. Age estimation and longevity in reptiles. *Gerontology* 40:174-192.

1031 Castanet J. 2006. Time recording in bone microstructures of endothermic animals; functional
1032 relationships. *Comptes Rendus Palevol* 5:629-636.

1033 Castanet J, and Baez M. 1991. Adaptation and evolution in Gallotia lizards from the Canary
1034 Islands: age, growth, maturity and longevity. *Amphibia-Reptilia* 12:81-102.

1035 Castanet J, Croci S, Aujard F, Perret M, Cubo J, and de Margerie E. 2004. Lines of arrested
1036 growth in bone and age estimation in a small primate: *Microcebus murinus*. *Journal of*
1037 *Zoology* 263:31-39.

1038 Castanet J, Curry Rogers KA, Cubo J, and Boisard J-J. 2000. Periosteal bone growth rates in
1039 extant ratites (ostriche and emu). Implications for assessing growth in dinosaurs. *Comptes*
1040 *Rendus de l'Academie des sciences, Series III, Sciences de la Vie* 323:543-550.

1041 Castanet J, and Smirina EM. 1990. Introduction to the skeletochronological method in
1042 amphibians and reptiles. *Annales des sciences naturelles, Zoologie* 11:191-196.

1043 Chávez-Aponte EO, Alfonzo-Hernández I, Finol HJ, Barrios N. CE, Boada-Sucre A, and
1044 Carrillo-Briceño JD. 2008. Histologia y ultraestructura de los osteodermos fosiles de *Glyptodon*
1045 *clavipes* y *Holmesina* sp. (Xenarthra: Cingulata). *Interciencia* 33:616-619.

1046 Chinsamy A, and Abdala F. 2008. Palaeobiological implications of the bone microstructure of
1047 South American traversodontids (Therapsida: Cynodontia). *South African Journal of*
1048 *Science* 104:225-230.

1049 Chinsamy A, and Hurum JH. 2006. Bone microstructure and growth patterns of early
1050 mammals. *Acta Palaeontologica Polonica* 51:325-338.

1051 Chinsamy A, Rich T, and Vickers-Rich P. 1998. Polar dinosaur bone histology. *Journal of*
1052 *Vertebrate Paleontology* 18:385-390.

1053 Chinsamy A, and Rubidge BS. 1993. Dicynodont (Therapsida) bone histology: phylogenetic and
1054 physiological implications. *Palaeontologia africana* 30:97-102.

1055 Chinsamy-Turan A. 2005. *The microstructure of dinosaur bone: Deciphering biology with fine*
1056 *scale techniques*. Baltimore: Johns Hopkins University Press.

1057 Chinsamy-Turan A. 2012a. Forerunners of mammals: radiation, histology, biology. Life of the
1058 past. Bloomington: Indiana University Press. p 352.

1059 Chinsamy-Turan A. 2012b. Microstructure of bones and teeth of nonmammalian therapsids. In:
1060 Chinsamy-Turan A, ed. *Forerunners of mammals: radiation, histology, biology*. Bloomington:
1061 Indiana University Press, 65-88.

1062 Clément G, and Geffard-Kuriyama D. 2010. Imaging and 3D in palaeontology and
1063 palaeoanthropology. *Comptes Rendus Palevol* 9:259–264.

1064 Cook SF, Brooks ST, and Ezra-Cohn HE. 1962. Histological studies on fossil bone. *Journal of*
1065 *Paleontology* 36:483-494.

1066 Cooper LN, Seiffert ER, Clementz M, Madar SI, Bajpai S, Hussain ST, and Thewissen JGM.
1067 2014. Anthracobunids from the middle eocene of India and pakistan are stem
1068 perissodactyls. *PloS one* 9:e109232.

1069 Cooper LN, Thewissen JGM, S. Bajpai S, and Tiwari BN. 2012. Postcranial morphology and
1070 locomotion of the Eocene raoellid *Indohyus* (Artiodactyla: Mammalia). *Historical*
1071 *Biology* 24:279-310.

1072 Cormack D. H. 1987. *Ham's histology*. Philadelphia: J. B. Lippincott Company.

1073 Crowder C, and Stout S. 2012. *Bone histology: an anthropological perspective*. Boca Raton:
1074 CRC Press.

1075 Cubo J, Legendre P, Ricqlès A de, Montes L, Margerie E de, Castanet J, and Desdevise Y. 2008.
1076 Phylogenetic, functional and structural components of variation in bone growth rate in
1077 amniots. *Evolution and Development* 10:217-227.

1078 Cubo J, Ponton F, Laurin M, Margerie E de, and Castanet J. 2005. Phylogenetic signal in bone
1079 microstructure of sauropsids. *Systematic Biology* 54:562–574.

1080 Cuijpers A. 2006. Histological identification of bone fragments in archaeology: telling humans
1081 apart from horses and cattle. *International Journal of Osteoarchaeology* 16 465–480.

1082 Curtin AJ, Macdowell AA, Schaible EG, and Roth L. 2012. Noninvasive histological
1083 comparison of bone growth patterns among fossil and extant neonatal elephantids using
1084 synchrotron radiation X-ray microtomography. *Journal of Vertebrate Paleontology* 32:939-955.

1085 Da Costa Pereira PVLG, Victer GD, Porpino KDO, and Bergqvist LP. 2012. Osteoderm
1086 histology of Late Pleistocene cingulates from the intertropical region of Brazil. *Acta*
1087 *Palaeontologica Polonica* 59:543-552.

1088 Deméré TA. 1994. Two new species of fossil walruses (Pinnipedia: Odobenidae) from the upper
1089 Pliocene San Diego Formation, California. *Proceedings of the San Diego Society of Natural*
1090 *History* 29:77-98.

1091 Drusini AZ. 1987. Refinement of two methods for the histomorphometric determination of age
1092 in human bone. *Zeitschrift für Morphologie und Anthropologie* 77:167-176.

1093 Dumont M, Laurin M, Jacques F, Pellé E, Dabin W, and Buffrénil V de. 2013. Inner architecture
1094 of vertebral centra in terrestrial and aquatic mammals: a two-dimensional comparative
1095 study. *Journal of Morphology* 274:570-584.

1096 Enlow DH. 1962. A study of the postnatal growth and remodeling of bone. *American Journal of*
1097 *Anatomy* 110:79-101.

1098 Enlow DH. 1969. The bone of reptiles. In: Gans C, Bellairs AdA, and Parsons TS, eds. *Biology*
1099 *of the Reptilia Vol 1 Morphology A*: Academic Press, London, 45-80.

1100 Enlow DH, and Brown SO. 1957. A comparative histological study of fossil and recent bone
1101 tissues. Part II. *Texas Journal of science* 9:186-214.

1102 Enlow DH, and Brown SO. 1958. A comparative histological study of fossil and recent bone
1103 tissues. Part III. *Texas Journal of science* 10:187-230.

1104 Erickson GM. 2014. On dinosaur growth. *Annual Review of Earth and Planetary*
1105 *Sciences* 42:675-697.

1106 Erickson GM, Curry Rogers K, and Yerby SA. 2001. Dinosaurian growth patterns and rapid
1107 avian growth rates. *Nature* 412:429-433.

1108 Erickson GM, Makovicky PJ, Currie PJ, Norell MA, Yerby SA, and Brochu CA. 2004.
1109 Gigantism and comparative life-history parameters of tyrannosaurid dinosaurs. *Nature* 430:772-
1110 775.

1111 Ezra HC, and Cook SF. 1959. Histology of mammoth bone. *Science* 129 465–466.

1112 Forasiepi AM, Cerdeño E, Bond M, Schmidt GI, Naipauer M, Straehl FR, Martinelli AG,
1113 Garrido AC, Schmitz MD, and Crowley JL. 2014. New toxodontid (Notoungulata) from the
1114 Early Miocene of Mendoza, Argentina. *Paläontologische Zeitschrift* DOI 10.1007/s12542-014-
1115 0233-5.

1116 Francillon-Vieillot H, Buffrénil V de, Castanet J, Géraudie J, Meunier FJ, Sire JY, and Ricqlès A
1117 de. 1990. Microstructure and mineralization of vertebrate skeletal tissues. In: Carter JG, editor.
1118 Skeletal Biomineralization: Patterns, Processes and Evolutionary Trends. New York: Van
1119 Nostrand Reinhold. p 471–530.

1120 Frylestam B, and von Schantz T. 1977. Age determination of European hares based on periosteal
1121 growth lines. *Mammal Review* 7:151-154.

1122 Garcia-Martinez R, Marin-Moratalla N, Jordana X, and Köhler M. 2011. The ontogeny of bone
1123 growth in two species of dormice: Reconstructing life history traits. *Comptes Rendus*
1124 *Palevol* 10:489-498.

1125 Geiger M, Wilson LAB, Costeur L, Sánchez R, and Sánchez-Villagra MR. 2013. Diversity and
1126 body size in giant caviomorphs (Rodentia) from the Northern Neotropics—study of femoral
1127 variation. *Journal of Vertebrate Paleontology* 33:1449-1456.

1128 Germain D, and Laurin M. 2005. Microanatomy of the radius and lifestyle in amniotes
1129 (Vertebrata, Tetrapoda). *Zoologica Scripta* 34:335-350.

1130 Gray NM, Kainec K, Madar S, Tomko L, and Wolfe S. 2007. Sink or Swim? Bone density as a
1131 mechanism for buoyancy control in early cetaceans. *Anatomical Record* 290:638-653.

1132 Green JL, M. H. Schweitzer MH, and Lamm E-T. 2010. Limb bone histology and growth
1133 in *Placerias hesternus* (Therapsida: Anomodontia) from the Upper Triassic of North
1134 America. *Palaeontology* 53:347-364.

1135 Griebeler EM, Klein N, and Sander PM. 2013. Aging, maturation and growth of
1136 sauropodomorph dinosaurs as deduced from growth curves using long bone histological data: an
1137 assessment of methodological constraints and solutions. *PloS one* 8: e67012.

1138 Gross W. 1934. Die Typen des mikroskopischen Knochenbaues bei fossilen Stegocephalen und
1139 Reptilien. *Zeitschrift für Anatomie und Enwicklungsgeschichte* 103:731-764.

1140 Habermehl K-H. 1985. *Altersbestimmung bei Wild- und Pelztieren - Möglichkeiten und*
1141 *Methoden - Ein praktischer Leitfaden für Jäger, Biologen und Tierärzte*. Hamburg, Berlin:
1142 Verlag Paul Parey.

1143 Hayashi S, Houssaye A, Nakajima Y, Chiba K, Ando T, Sawamura H, Inuzuka N, Kaneko N,
1144 and Osaki T. 2013. Bone inner structure suggests increasing aquatic adaptations in Desmostylia
1145 (Mammalia, Afrotheria). *PloS one* 8:e59146.

1146 Herdina AN, Herzig-Straschil B, Hilgers H, Metscher BD, and Plenk HJ. 2010.
1147 Histomorphology of the penis bone (baculum) in the gray long-eared bat *Pleocotus*
1148 *austriacus* (Chiroptera, Vespertilionidae). *The Anatomical Record* 293:1248–1258.

1149 Hill RV. 2006. Comparative anatomy and histology of xenarthran osteoderms. *Journal of*
1150 *Morphology* 267:1441-1460.

1151 Hillier ML, and Bell LS. 2007. Differentiating human bone from animal bone: A review of
1152 histological methods. *Journal of Forensic Sciences* 52:249−263.

1153 Hillier ML, and Bell LS. 2007. Differentiating human bone from animal bone: a review of
1154 histological methods. *Journal of Forensic Sciences* 52:249−263.

1155 Hofmann R, Stein K, and Sander PM. 2014. Constraints on the lamina density of laminar bone
1156 architecture of large-bodied dinosaurs and mammals. *Acta Palaeontologica Polonica* 59 287-
1157 294.

1158 Horner JR, Ricqlès A de, and Padian K. 1999. Variation in dinosaur skeletochronology
1159 indicators: implications for age assessment and physiology. *Paleobiology* 25:295-304.

1160 Horner JR, Ricqlès A de, and Padian K. 2000. Long bone histology of the hadrosaurid
1161 dinosaur *Maiasaura peeblesorum*: growth dynamics and physiology based on an ontogenetic
1162 series of skeletal elements. *Journal of Vertebrate Paleontology* 20:115-129.

1163 Horner JR, and Padian K. 2004. Age and growth dynamics of *Tyrannosaurus rex*. *Proceedings of*
1164 *the Royal Society of London B* 271:1875-1880.

1165 Houssaye A, P. T, Muizon C de, and Gingerich PD. 2015. Transition of Eocene whales from
1166 land to sea: evidence from bone microstructure. *PloS one* 10:e0118409.

1167 Huttenlocker AK. 2008. Comparative osteohistology of hyperelongate neural spines in basal
1168 synapsids (Vertebrata: Amniota): Growth and mechanical considerations MSc MSc thesis.
1169 California State University.

1170 Huttenlocker AK, and Botha-Brink J. 2013. Body size and growth patterns in the
1171 therocephalian *Moschorhinus kitchingi* (Therapsida: Eutheriodontia) before and after the end-
1172 Permian extinction in South Africa. *Paleobiology* 39:253–277.

1173 Huttenlocker AK, and Botha-Brink J. 2014. Bone microstructure and the evolution of growth
1174 patterns in Permo-Triassic therocephalians (Amniota, Therapsida) of South
1175 Africa. *PeerJ* 2:e325:1-31.

1176 Huttenlocker AK, Mazierski D, and Reisz RR. 2011. Comparative osteohistology of
1177 hyperelongate neural spines in the Edaphosauridae (Amniota:
1178 Synapsida). *Palaeontology* 54:573-590.

1179 Huttenlocker AK, and Rega E. 2012. The paleobiology and bone microstructure of
1180 pelycosaurian-grade synapsids. In: Chinsamy-Turan A, ed. *Forerunners of mammals: radiation,*
1181 *histology, biology*. Bloomington: Indiana University Press, 91-119.

1182 Huttenlocker AK, Rega E, and Sumida SS. 2010. Comparative anatomy and osteohistology of
1183 hyperelongate neural spines in the sphenacodontids *Sphenacodon* and *Dimetrodon* (Amniota:
1184 Synapsida). *Journal of Morphology* 271:1407-1421.

1185 Huttenlocker AK, Woodward HN, and Hall BK. 2013. The biology of bone. In: Padian K, and
1186 Lamm E-T, eds. *Histology of fossil tetrapods - Advancing methods, analysis and interpretation*.
1187 Berkeley, Los Angeles, London: University of California Press, 13-34.

1188 Jasinoski SC, Rayfield EJ, and Chinsamy A. 2010a. Functional implications of dicynodont
1189 cranial suture morphology. *Journal of Morphology* 271:705-728.

1190 Jasinoski SC, Rayfield EJ, and Chinsamy A. 2010b. Mechanics of the scarf premaxilla-nasal
1191 suture in the snout of *Lystrosaurus*. *Journal of Vertebrate Paleontology* 30:1283-1288.

1192 Johnston DH, and Beauregard M. 1969. Rabies epidemiology in Ontario. *Bulletin of the Wildlife*
1193 *Disease Association* 5:357-370.

1194 Kaiser HE. 1960. Untersuchungen zur vergleichenden Osteologie der fossilen und rezenten
1195 Pachyostosen. *Palaeontographica Abteilung A* 114:113-196.

1196 Kerley ER. 1965. The microscopic determination of age in human bone. *American Journal of*
1197 *Physical Anthropology* 23:149–163.

1198 Kielan−Jaworowska Z, Cifelli RL, and Luo XZ. 2004. *Mammals from the age of dinosaurs:*
1199 *origins, evolution, and structure*. New York: Columbia University Press.

1200 King CM. 1991. A review of age determination methods for the stoat *Mustela erminea*. *Mammal*
1201 *Review* 21:31-49.

1202 Kiprijanoff W. 1883. Studien über die fossilien Reptilien Russlands. IV. Theil. Ordnung
1203 Grocodilina Oppel. *Mémoires de l'Académie des Sciences de St-Pétersbourg, VIIe Série Tome*
1204 *XXXI* 7:1-29.

1205 Klein N, and Sander PM. 2008. Ontogenetic stages in the long bone histology of sauropod
1206 dinosaurs. *Paleobiology* 34:247-263.

1207 Klevezal GA. 1996. *Recording structures of mammals. Determination of age and reconstruction*
1208 *of life history*. Rotterdam/Brookfield: A.A.Balkema.

1209 Klevezal GA, and Kleinenberg SE. 1969. *Age determination of mammals from annual layers in*
1210 *teeth and bones*. Jerusalem: Israel Program of Scientific Translations.

1211 Köhler M, Marín-Moratalla N, Jordana X, and Aanes R. 2012. Seasonal bone growth and
1212 physiology in endotherms shed light on dinosaur physiology. *Nature* 487:358-361.

1213 Köhler M, and Moyà-Solà S. 2009. Physiological and life history strategies of a fossil large
1214 mammal in a resource-limited environment. *Proceedings of the National Academy of Sciences of*
1215 *the United States of America* 106:20354-20358.

1216 Kolb C, Scheyer TM, Lister AM, Azorit C, de Vos J, Schlingemann MAJ, Rössner GE,
1217 Monaghan NT, and Sánchez-Villagra MR. 2015. Growth in fossil and extant deer and
1218 implications for body size and life history evolution. *BMC Evolutionary Biology* 15:1-15.

1219 Kriloff A, Germain D, Canoville A, Vincent P, Sache M, and Laurin M. 2008. Evolution of bone
1220 microanatomy of the tetrapod tibia and its use in palaeobiological inference. *Journal of*
1221 *Evolutionary Biology* 21:807-826.

1222 Krmpotic CM, Ciancio MR, Barbeito CG, Mario RC, and Carlini AA. 2009. Osteoderm
1223 morphology in recent and fossil euphractine xenarthrans. *Acta Zoologica* 90:339-351.

1224 Laurin M. 2004. The evolution of body size. Cope's rule and the origin of amniotes. *Systematic*
1225 *Biology* 53:594-622.

1226 Laurin M, and Buffrénil V de. 2015. Microstructural features of the femur in early
1227 ophiacodontids: a reappraisal of ancestral habitat use and lifestyle of amniotes *Comptes Rendus*
1228 *Palevol*.

1229 Laurin M, Girondot M, and Loth M-M. 2004. The evolution of long bone microanatomy and
1230 lifestyle in lissamphibians. *Palaeobiology* 30:589-613.

1231 Lee AH, Huttenlocker AK, Padian K, and Woodward HN. 2013. Analysis of growth rates. In:
1232 Padian K, and Lamm E-T, eds. *Bone histology of fossil tetrapods*. Berkeley: University of
1233 California Press, 217-251.

1234 Lee AH, and Werning S. 2008. Sexual maturity in growing dinosaurs does not fit reptilian
1235 growth models. *Proceedings of the National Academy of Sciences of the United States of*
1236 *America* 105:582-587.

1237 Lomolino MV, Sax DF, Palombo MR, and van der Geer AA. 2012. Of mice and mammoths:
1238 evaluations of causal explanations for body size evolution in insular mammals. *Journal of*
1239 *Biogeography* 39:842-854.

1240 Lomolino MV, van der Geer AA, Lyras GA, Palombo MR, Sax DF, and Rozzi R. 2013. Of mice
1241 and mammoths: generality and antiquity of the island rule. *Journal of Biogeography* 40:1427-
1242 1439.

1243 Luo XZ. 2011. Developmental Patterns in Mesozoic Evolution of Mammal Ears. *Annual Review*
1244 *of Ecology, Evolution, and Systematics* 42:355-380

1245 Luo ZX, and Wible JR. 2005. A Late Jurassic digging mammal and early mammalian
1246 diversification. *Science* 308:103-107.

1247 Maddison WP, and Maddison DR. 2015. Mesquite: a modular system for evolutionary analysis.
1248 Version 3.02. *Available at http://mesquiteproject.org.*

1249 Mahboubi S, Bocherens H, Scheffler M, Benammi M, and Jaeger JJ. 2014. Was the Early
1250 Eocene proboscidean *Numidotherium koholense* semi-aquatic or terrestrial? Evidence from
1251 stable isotopes and bone histology. *Comptes Rendus Palevol* 13:501–509.

1252 Marangoni F, Schaefer E, Cajade R, and Tejedo M. 2009. Growth mark formation and
1253 chronology of two neotropical anuran species. *Journal of Herpetology* 43:546-550.

1254 Margerie E de, Cubo J, and Castanet J. 2002. Bone typology and growth rate: Testing and
1255 quantifying 'Amprino's rule' in the mallard (*Anas platyrhynchus*). *Comptes Rendus*
1256 *Biologies* 325:221-230.

1257 Margerie E de, Robin JP, Verrier D, Cubo J, Groscolas R, and Castanet J. 2004. Assessing a
1258 relationship between bone microstructure and growth rate: a fluorescent labelling study in the
1259 king penguin chick (*Aptenodytes patagonicus*). *Journal of Experimental Biology* 207:869-879.

1260 Marin-Moratalla N, Cubo J, Jordana X, Moncunill-Solè B, and Köhler M. 2014. Correlation of
1261 quantitative bone histology data with life history and climate: a phylogenetic
1262 approach. *Biological Journal of the Linnean Society* 112:678-687.

1263 Marin-Moratalla N, Jordana X, and Köhler M. 2013. Bone histology as an approach to providing
1264 data on certain key life history traits in mammals: Implications for conservation
1265 biology. *Mammalian Biology* 78:422-429.

1266 Martínez-Maza C, Rosas A, and García-Vargas S. 2006. Bone paleohistology and human
1267 evolution. *Journal of Anthropological Sciences* 84:33-52.

1268 Martinez-Maza C, Rosas A, Garcia-Vargas S, Estalrrich A, and de la Rasilla M. 2011. Bone
1269 remodelling in Neanderthal mandibles from the El Sidron site (Asturias, Spain). *Biology*
1270 *Letters* 7:593e596.

1271 Martiniaková M, Grosskopf B, Vondráková M, Omelka R, and Fabiš M. 2005. Observation of
1272 the microstructure of rat cortical bone tissue. *Scripta Medica* 78:45-50.

1273 McNab B. 1994. Resource use and the survival of land and freshwater vertebrates on oceanic
1274 islands. *The American Naturalist* 144:643-660.

1275 McNab BK. 2002. Minimizing energy expenditure facilitates vertebrate persistence on oceanic
1276 islands. *Ecological Letters* 5:693-704.

1277 McNab BK. 2010. Geographic and temporal correlations of mammalian size reconsidered: a
1278 resource rule. *Oecologia* 164:13-23.

1279 Meier PS, Bickelmann C, Scheyer, Koyabu D, and Sánchez-Villagra MR. 2013. Evolution of
1280 bone compactness in extant and extinct moles (Talpidae): exploring humeral microstructure in
1281 small fossorial mammals. *BMC Evolutionary Biology* 13:55.

1282 Meredith RW, Janecka J, Gatesy J, Ryder OA, Fisher CA, Teeling EC, Goodbla A, Eizirik E,
1283 Simão TLL, Stadler T, Rabosky DL, Honeycutt RL, Flynn JJ, Ingram CM, Steiner C, Williams
1284 TL, Robinson TJ, Burk-Herrick A, Westerman M, Ayoub NA, Springer MS, and Murphy WJ.
1285 2011. Impacts of the Cretaceous terrestrial revolution and KPg extinction on mammal
1286 diversification. *Science* 334:521-524.

1287 Mitchell EDJ. 1963. Brachydont desmostylian from Miocene of San Clemente Island,
1288 California. *Bulletin of the Southern California Academy of Science* 62:192-201.

1289 Mitchell EDJ. 1964. Pachyostosis in desmostylids. *The Geological Society of America Special*
1290 *Paper* 76:214.

1291 Mitchell J, and Sander PM. 2014. The three-front model: a developmental explanation of long
1292 bone diaphyseal histology of Sauropoda. *Biological Journal of the Linnean Society* 112:765–
1293 781.

1294 Morris P. 1970. A method for determining absolute age in the hedgehog. *Journal of*
1295 *Zoology* 161:277-281.

1296 Musser AM, and Archer M. 1998. New information about the skull and dentary of the
1297 Miocene *Platypus obdurodon dicksoni*, and a discussion of ornithorhynchid
1298 relationships. *Philosophical Transactions of the Royal Society of London B* 353:1063-1079.

1299 Nasterlack T, Canoville A, and Chinsamy A. 2012. New insights into the biology of the Permian
1300 genus *Cistecephalus* (Therapsida, Dicynodontia). *Journal of Vertebrate Paleontology* 32:1396-
1301 1410.

1302 Nopcsa F von, and Heidsieck E. 1933. On the histology of the ribs of immature and half-grown
1303 trachodont dinosaurs. *Proceedings of the Zoological Society of London* 1:221-223.

1304 Nopcsa F von, and Heidsieck E. 1934. Über eine pachyostotische Rippe aus der Kreide Rügens.
1305 *Acta Zoologica* 15:431-455.

1306 O'Leary MA, Bloch JI, Flynn JJ, Gaudin TJ, Giallombardo A, Giannini NP, Goldberg SL,
1307 Kraatz BP, Luo Z-X, Meng J, Ni X, Novacek MJ, Perini FA, Randall ZS, Rougier GW, Sargis
1308 EJ, Silcox MT, Simmons NB, Spaulding M, Velazco PM, Weksler M, Wible JR, and Cirranello
1309 AL. 2013. The Placental Mammal Ancestor and the Post-K-Pg Radiation of
1310 Placentals. *Science* 339:662-667.

1311 O'Leary MA, and Kaufman SG. 2012. MorphoBank 3.0: web application for morphological
1312 phylogenetics and taxonomy. *Available at http://www.morphobank.org* (accessed 6 May 2015).

1313 Padian K. 2011. Vertebrate palaeohistology then and now: A retrospective in the light of the
1314 contributions of Armand de Ricqles. *Comptes Rendus Palevol* 10:303-309.

1315 Padian K. 2013. Book review: forerunners of mammals: radiation, histology, biology. *Journal of*
1316 *Vertebrate Paleontology* 33:1250-1251.

1317 Padian K, and Lamm E-T. 2013. Bone histology of tetrapods. Berkeley, Los Angeles: University
1318 of California Press. p 285.

1319 Pascal M, and Castanet J. 1978. Méthodes de la détermination de l'age chez le chat haret des iles
1320 Kerguelen. *Terre et Vie* 32:529-554.

1321 Pascal M, and Delattre P. 1981. Comparaison des différentes méthodes de la détermination de
1322 l'age individuel chez le vison (*Mustela vison* Schreber). *Canadian Journal of Zoology* 59:202-
1323 211.

1324 Pascual R, Archer M, Jaureguizar EO, Prado JL, Godthelp H, and Hand SJ. 1992. First discovery
1325 of monotremes in South America. *Nature* 356:704 - 706.

1326 Pazzaglia UE, Sibilia V, Congiu T, Pagani F, Ravanelli M, and Zarattini G. 2015. Setup of a
1327 bone aging experimental model in the rabbit comparing changes in cortical and trabecular bone:
1328 morphological and morphometric study in the femur. *Journal of Morphology*.

1329 Peabody FE. 1961. Annual growth zones in living and fossil vertebrates. *Journal of*
1330 *Morphology* 108:11-62.

1331 Ponton F, Elzanowski A, Castanet J, Chinsamy A, Margerie E de, Ricqlès A de, and Cubo J.
1332 2004. Variation of the outer circumferential layer in the limb bones of birds. *Acta*
1333 *Ornithologica* 39:21-24.

1334 Prondvai E, Stein KHW, Ricqlès A de, and Cubo J. 2014. Development-based revision of bone
1335 tissue classification: the importance of semantics for science. *Biological Journal of the Linnean*
1336 *Society* 112:799-816.

1337 Quekett JT. 1849a. On the intimate structure of bone as composing the skeleton in the four great
1338 classes of animals, viz., mammals, birds, reptiles, and fishes, with some remarks on the great
1339 value of the knowledge of such structure in determining the affinities of minute fragments of
1340 organic remains. *Transactions of the Microscopical Society of London* 2:46-58.

1341 Quekett JT. 1849b. Additional observations on the intimate structure of bone. *Transactions of the*
1342 *Microscopical Society of London* 2:59-64.

1343 Quekett JT. 1855. *Descriptive and illustrated catalogue of the histological series contained in*
1344 *the museum of the Royal College of Surgeons of England. Volume II. Structure of the skeleton of*
1345 *vertebrate animals*. London: Taylor and Francis.

1346 Raia P, Barbera C, and Conte M. 2003. The fast life of a dwarfed giant. *Evolutionary*
1347 *Ecology* 17:293-312.

1348 Ray S, Bandyopadhyay S, and Appana R. 2010. Bone histology of a kannemeyeriid
1349 dicynodont *Wadiasaurus*: palaeobiological implications. In: Bandyopadhyay S, ed. *New aspects*
1350 *of mesozoic biodiversity*. Heidelberg: Springer, 73-89.

1351 Ray S, Botha J, and Chinsamy A. 2004. Bone histology and growth patterns of some
1352 nonmammalian therapsids. *Journal of Vertebrate Paleontology* 24:634-648.

1353 Ray S, Botha-Brink J, and Chinsamy-Turan A. 2012. Microstructure of bones and teeth of
1354 nonmammalian therapsids. In: Chinsamy-Turan A, ed. *Forerunners of mammals: radiation,*
1355 *histology, biology*. Bloomington: Indiana University Press, 121-146.

1356 Ray S, and Chinsamy A. 2004. *Diictodon feliceps* (Therapsida, Dicynodontia): bone histology,
1357 growth, and biomechanics. *Journal of Vertebrate Paleontology* 24:180-194.

1358 Ray S, Chinsamy A, and Bandyopadhyay S. 2005. *Lystrosaurus murrayi* (Therapsida,
1359 Dicynodontia): bone histology, growth and lifestyle adaptations. *Palaeontology* 48:1169-1185.

1360 Rega E, Sumida SS, Noriega K, Pell C, and Lee A. 2005. Evidence-based paleopathology I:
1361 ontogenetic and functional implications of dorsal sails in *Dimetrodon*. *Journal of Vertebrate*
1362 *Paleontology* 25:103A.

1363 Ricqlès A de. 1969. Recherches palèohistologiques sur les os longs des tetrapodes. II.- Quelques
1364 observations sur la structure des os longs des thériodontes. *Annales de Paléontologie* 55:1-52.

1365 Ricqlès A de. 1972. Recherches palèohistologiques sur les os longs des tetrapodes. III.-
1366 Titanosuchiens, dinocéphaliens et dicynodontes. *Annales de Paléontologie (Vertébrés)* 58:17-46.

1367 Ricqlès A de. 1974a. Evolution of endothermy: histological evidence. *Evolutionary Theory* 1:51-
1368 80.

1369 Ricqlès A de. 1974b. Recherches paléohistologiques sur les os longs des tétrapodes. IV. -
1370 Éothériodontes et pélycosaures. *Annales de Paléontologie* 60:1-56.

1371 Ricqlès A de. 1975. Recherches paléohistologiques sur les os longs des tétrapodes VII. - Sur la
1372 classification, la signification fonctionnelle et l'histoire des tissus oseux des tétrapodes. Première
1373 partie, structures. *Annales de paléontologie 61, 51-129* 61:51-129.

1374 Ricqlès A de. 1976a. On bone histology of fossil and living reptiles, with comments on its
1375 functional and evolutionary significance. In: Bellairs A, and Cox CB, eds. *Morphology and*
1376 *Biology of Reptiles*. London and New York: Academic Press, 123-150.

1377 Ricqlès A de. 1976b. Recherches paléohistologiques sur les os longs des tétrapodes. VII. - Sur la
1378 classification, la signification fonctionnelle et l'histoire des tissus osseux des tétrapodes.
1379 Deuxième partie. Fonctions: considérations fonctionnelles et physiologiques. *Annales de*
1380 *Paléontologie* 62:71-126.

1381 Ricqlès A de. 1978. Recherches paléohistologiques sur les os longs des tétrapodes. VII. — Sur la
1382 classification, la signification fonctionnelle et l'histoire des tissus osseux des tétrapodes.
1383 Troisième partie. IV.-Les problèmes du déterminisme des types de tissus osseux. *Annales de*
1384 *Paléontologie* 64:153-184.

1385 Ricqlès A de, and Buffrénil V de. 1995. Sur la présence de pachyostéosclerosis chez la rhytine
1386 de Steller (*Rhytina* (*Hydrodamalis*) *gigas*), sirénian rézent éteint. *Annales des Sciences*
1387 *Naturelles, Zoologie, Paris, 13e Série* 16:47-53.

1388 Ricqlès A de, Castanet J, and Francillon-Vieillot H. 2004. The "message" of bone tissue in
1389 Palaeoherpetology. *Italian Journal of Zoology*:3-12.

1390 Ricqlès A de, and Cubo J. 2010. Le problème de la causalité complexe aux sources de la relation
1391 structuro-fonctionnelle : 1/généralités, 2/l'exemple du tissu osseux. In: Gayon J, and Ricqlès Ad,
1392 eds. *Les Fonctions : des organismes aux artefacts*. Paris: PUF, 179-188.

1393 Ricqlès A de, Meunier FJ, Castanet J, and Francillon-Vieillot H. 1991. Comparative
1394 microstructure of bone. In: Hall BK, ed. *Bone Volume 3: Bone matrix and bone specific*
1395 *products*. Boca Raton: CRC Press, 1-78.

1396 Ricqlès A de, Taquet P, and Buffrenil V de. 2009. “Rediscovery” of Paul Gervais'
1397 paleohistological collection. *Geodiversitas* 31:943-971.

1398 Ricqlès A de. 2011. Vertebrate palaeohistology: past and future. *Comptes Rendus*
1399 *Palevol* 10:509–515.

1400 Romer AS. 1957. Origin of the amniote egg. *Scientific monthly* 85:57-63.

1401 Romer AS. 1958. Tetrapod limbs and early tetrapod life. *Evolution* 12:365-369.

1402 Rubidge BS, and Sidor CA. 2001. Evolutionary patterns among Permo-Triassic
1403 therapsids. *Annual Review of Ecology and Systematics* 32:449-480.

1404 Ryan TM, and Shaw CN. 2015. Gracility of the modern *Homo sapiens* skeleton is the result of
1405 decreased biomechanical loading. *Proceedings of the National Academy of Sciences of the*
1406 *United States of America* 112:372-377.

1407 Sanchez S, Ahlberg P, Trinajstic K, Mirone A, and Tafforeau P. 2012. Three dimensional
1408 synchrotron virtual paleohistology: a new insight into the world of fossil bone
1409 microstructures. *Microscopy and Microanalysis* 18:1095-1105.

1410 Sander PM. 2000. Longbone histology of the Tendaguru sauropods: implications for growth and
1411 biology. *Paleobiology* 26:466-488.

1412 Sander PM, and Andrassy P. 2006. Lines of arrested growth and long bone histology in
1413 Pleistocene large mammals from Germany: What do they tell us about dinosaur
1414 physiology? *Palaeontographica Abteilung A* 277:143-159.

1415 Sander PM, Klein N, Buffetaut E, Cuny G, Suteethorn V, and Le Loeuff J. 2004. Adaptive
1416 radiation in sauropod dinosaurs: bone histology indicates rapid evolution of giant body size
1417 through acceleration. *Organisms, Diversity & Evolution* 4:165-173.

1418 Sander PM, and Tückmantel C. 2003. Bone lamina thickness, bone apposition rates, and age
1419 estimates in sauropod humeri and femora. *Paläontologische Zeitschrift* 77:161-172.

1420 Schaffer J. 1890. Über den feineren Bau fossiler Knochen. *Sitzungsberichte der Kaiserlichen*
1421 *Akademie der Wissenschaften* Mathematisch-Naturwissenschaftliche Classe XCVIII. Band.
1422 Hefte I bis X. Abtheilung III:319-382.

1423 Scheyer TM. 2009-2015. Palaeohistology. In: Sánchez-Villagra MR, editor. Developmental -
1424 Palaeontology net. Zurich: Palaeontological Institute of the University of Zurich. *Available at*
1425 *http://www.developmental-palaeontology.net/palaeohistology/index.php* (accessed 1 June 2015).

1426 Scheyer TM, Klein N, and Sander PM. 2010. Developmental palaeontology of Reptilia as
1427 revealed by histological studies. *Seminars in Cell & Developmental Biology* 21:462-470.

1428 Schultz M. 1997. Microscopic investigation of excavated skeletal remains: a contribution to
1429 paleopathology and forensic medicine. In: Haglund WD, and Sorg MH, eds. *Forensic taphonomy*
1430 *The postmortem fate of human remains*. Boca Raton/New York/London/Tokyo: CRC Press, 201-
1431 222.

1432 Schultz M, and Schmidt-Schultz TH. 2014. Microscopic research on fossil human bone. In:
1433 Henke W, and Tattersall I, eds. *Handbook of paleoanthropology*. 2nd ed. Heidelberg/New York:
1434 Springer, 983-998.

1435 Shelton C, and Sander PM. 2015. *Ophiacodon* long bone histology: the earliest occurrence of
1436 FLB in the mammalian stem lineage. *PeerJ PrePrints* Available
1437 at https://dx.doi.org/10.7287/peerj.preprints.1027v1 (accessed 11 May 2015).

1438 Shelton CD, Sander PM, Stein K, and Winkelhorst H. 2013. Long bone histology indicates
1439 sympatric species of Dimetrodon (Lower Permian, Sphenacodontidae). *Earth and Environmental*
1440 *Science Transactions of the Royal Society of Edinburgh* 103:1-20.

1441 Sigurdsen T, Huttenlocker AK, Modesto SP, Rowe T, and Damiani R. 2012. Reassessment of the
1442 morphology and paleobiology of the therocephalian *Tetracynodon darti* (Therapsida), and the
1443 phylogenetic relationships of Baurioidea. *Journal of Vertebrate Paleontology* 32:1113-1134.

1444 Singh IJ, Tonna EA, and Gandel CP. 1974. A comparative histological study of mammalian
1445 bone. *Journal of Morphology* 144:421-438.

1446 Skinner MM, Stephens NB, Tsegai ZJ, Foote AC, Nguyen NH, Gross T, Pahr DH, Hublin J-J,
1447 and Kivell TL. 2015. Human-like hand use in *Australopithecus africanus*. *Science* 347:395–399.

1448 Stein K, and Prondvai E. 2013. Rethinking the nature of fibrolamellar bone: an integrative
1449 biological revision of sauropod plexiform bone formation. *Biological Reviews*:1-24.

1450 Stein K, and Sander M. 2009. Histological core drilling: a less destructive method for studying
1451 bone histology. First Annual Fossil Preparation and Collections Symposium. Petrified Forest
1452 National Park: Petrified Forest. p 69-80.

1453 Straehl FR, Scheyer TM, Forasiepi AM, MacPhee RD, and Sánchez-Villagra MR. 2013.
1454 Evolutionary patterns of bone histology and bone compactness in xenarthran mammal long
1455 bones. *Plosone* 8:e69275.

1456 Tacutu R, Craig T, Budovsky A, Wuttke D, Lehmann G, Taranukha D, Costa J, Fraifeld VE, and
1457 de Magalhaes JP. 2013. Human Ageing Genomic Resources: Integrated databases and tools for
1458 the biology and genetics of ageing. *Nucleic Acids Research* 41:D1027-D1033.

1459 Thewissen JGM, Cooper LN, Clementz MT, Bajpai S, and Tiwari BN. 2007. Whales originated
1460 from aquatic artiodactyls in the Eocene epoch of India. *Nature* 450:1190-1194.

1461 Tomassini RL, Montalvo CI, Manera T, and Visconti G. 2014. Mineralogy, geochemistry, and
1462 paleohistology of pliocene mammals from the Monte Hermoso Formation (Argentina).
1463 *Paedotherium bonaerense* (Notoungulata, Hegetotheriidae) as a case study. *Ameghiniana*
1464 51:385-395.

1465 van der Geer A, Lyras G, de Vos J, and Dermitzakis M. 2010. *Evolution of island mammals.*
1466 *Adaptation and extinction of placental mammals on islands*. Sussex: Wiley-Blackwell.

1467 Vanderhoof VL. 1937. A study of the Miocene sirenian *Desmostylus*. *University of California*
1468 *Publications in the Geological Sciences* 24:169-262.

1469 Vickaryous MK, and Hall BK. 2006. Osteoderm morphology and development in the nine-
1470 banded armadillo, *Dasypus novemcinctus* (Mammalia, Xenarthra, Cingulata). *Journal of*
1471 *Morphology* 267:1273-1283.

1472 Vickaryous MK, and Sire JY. 2009. The integumentary skeleton of tetrapods: origin, evolution,
1473 and development. *Journal of Anatomy* 214:441-464.

1474 Warren JW. 1963. Growth zones in the skeleton of recent and fossil vertebrates PhD. University
1475 of California.

1476 Wolf D. 2007. Osteoderm histology of extinct and recent Cingulata and Phyllophaga (Xenarthra,
1477 Mammalia): implications for systematics and biomechanical adaptation. *Hallesches Jahrbuch für*
1478 *Geowissenschaften* Beiheft 23:145-151.

1479 Wolf D. 2008. Osteoderm histology of the Cingulata (Xenarthra, Mammalia): implications for
1480 systematics. *Journal of Vertebrate Paleontology* 28:161A.

1481 Wolf D, Kalthoff DC, and Martin Sander PM. 2012. Osteoderm histology of the Pampatheriidae
1482 (Cingulata, Xenarthra, Mammalia): implications for systematics, osteoderm growth, and
1483 biomechanical adaptation. *Journal of Morphology* 273:388-404.

1484 Woodward HN, Padian K, and Lee AH. 2013. Skeletochronology. In: Padian K, and Lamm E-T,
1485 eds. *Histology of fossil tetrapods - Advancing methods, analysis and interpretation*. Berkeley,
1486 Los Angeles, London: University of California Press, 195-215.

1487 Zedda M, Lepore G, Manca P, Chisu V, and Farina V. 2008. Comparative bone histology of
1488 adult horses and cows. *Journal of Veterinary Medicine Series C* 37:442–445.

1489 Zylberberg L, Traub W, Buffrénil V de, Allizard F, Arad T, and Weiner S. 1998. Rostrum of a
1490 toothed whale: ultrastructural study of a very dense bone. *Bone* 23:241-247.

1491

Figure captions

Figure 1: Typical mammalian bone tissue as observed in large mammals such as cervids. Red bars indicate area and plane of sectioning. Histological images B), E), and I) in linear polarised light, C) in crossed polarised light and with additional use of lambda compensator, and F) in crossed polarised light. A) Life reconstruction of the cervid *Megaloceros giganteus* ("Knight Megaloceros" by Charles R. Knight, courtesy of the American Museum of Natural History via Wikimedia Commons - http://commons.wikimedia.org). B, C) Bone cortex of a tibia of *Megaloceros giganteus* specimen NMING:F21306/14 displaying an endosteal lamellar layer (innermost part of the cortex) and reticular as well as plexiform fibrolamellar primary bone with growth marks. Note that the primary bone is pervaded by secondary Haversian systems in the inner third of the bone cortex. White arrows indicate lines of arrested growth. Occurrence of LAGs indicated by black/white arrows and the outer circumferential layer (OCL) by white brackets. D) Photograph of *Pudu puda* ("Pudupuda hem 8 FdoVidal Villarr 08Abr06-PhotoJimenez", courtesy of Jaime E. Jimenez via Wikimedia Commons - http://commons.wikimedia.org). E, F) Bone cortex of a femur of *Pudu puda* specimen NMW 60135 displaying an endosteal lamellar layer and mainly plexiform fibrolamellar bone. G) Reconstruction of *Paraceratherium* ("Indricotherium11", Courtesy of Dmitry Bogdanov via Wikimedia Commons - http://commons.wikimedia.org). H) Cross-section of a rib of *Paraceratherium* sp. specimen MTA-TTM 2006-1209. Red rectangle indicates area of dense Haversian bone magnified in I).

Figure 2: Phylogeny of basal synapsids focussing on groups discussed, based on Rubidge & Sidor (2001), Benson (2012), and Brink & Reisz (2014.

Figure 3: Phylogeny of Mammaliamorpha focussing on groups discussed, based on Luo et al. (2005), Luo et al. (2011), Meredith et al. (2011), and O'Leary et al. (2013). Notoungulates and Pantodonta are not included given their controversial systematic position.

Figure 4: Femoral bone cortex of marsupials. Histological images A) and D) in linear polarised light and B), C), E), and F) in crossed polarised light. A, B) Outer bone cortex of adult *Didelphis albiventris* specimen PIMUZ A/V 5279. Note the occurrence of simple primary longitudinal vascular canals and primary osteons in mainly parallel-fibred bone tissue. C) Inner bone cortex of the same specimen displaying a distinct endosteal lamellar layer. D, E) Bone cortex of adult *Lutreolina crassicautada* specimen PIMUZ A/V 5275. F) Inner cortex of same specimen. Note the occurrence of primary longitudinal vascular canals and primary osteons as well as Haversian systems within the parallel-fibred bone.

Figure 5: Histological features of the femur of *Deinogalerix* sp. A) Life reconstruction of *Deinogalerix koenigswaldi* in comparison to the extant hedgehog *Erinaceus* (modified from Agustí & Antón, 2002). B) Adult right femur (specimen RGM.178017) in anterior view. Red bar indicates area and plane of sectioning. C) Lateral bone cortex in crossed polarised light showing parallel-fibred bone and 5 LAGs. Occurrence of LAGs indicated by white arrows.

Figure 6: Bone cortex of *Hippopotamus minor* femora. A) Life reconstruction (from van der Geer et al., 2010; drawing: Alexis Vlachos) of another Mediterranean dwarf hippopotamid from the Middle Pleistocene of Crete. Since no life reconstruction of *Hippopotamus minor* is available, we here show the one of *Hippopotamus creutzburgi*. Histological images B), and C) in linear polarised light, D) in crossed polarised light. B)

Small juvenile specimen CKS 110/B. C) Intermediate sized juvenile specimen CKS 122/B showing reticular to plexiform vascularised bone. Note that the central part mainly consists of reticular bone. D) Outer bone cortex of large juvenile specimen CKS 117 showing mainly parallel-fibred bone. Black and grey areas indicate zones of recrystallisation due to diagenetic alteration of bone tissue.

Figure 7: Histological features of *Sinomegaceros yabei*, the megacerine deer from the Pleistocene of Japan. Histological images in linear polarised light of an adult femur (OMNH QV-4062) depicting A) the whole cross-section and B) a close-up of the outer cortex. The red bar in A) localizes the approximated position of the section on the life reconstruction (courtesy of Hirokazu Tokugawa), and the red rectangle indicates the area of the close-up. B) Note that seven LAGs are visible, as indicated by white arrows.

Figure 8: Bone histology of fossil island rodents. Histological images A) and D) in linear polarised light, B) and E) in crossed polarised light, and C) and F) in crossed polarised light with additional use of lambda compensator. A-C) Adult *Mikrotia* sp. femur (specimen RGM.792085) showing disorganised, parallel-fibred/lamellar bone in its centre. D-F) Adult femur of *Leithia* sp. specimen NMB G 2160 displaying lamellar bone being pervaded by longitudinal to radial primary osteons and irregularly shaped and partially oblique secondary osteons.

Figure 9: Bone histology of fossil ochotonids. A) Life reconstruction of *Prolagus sardus* ("Prolagus3", courtesy of Wikimedia Commons - http://commons.wikimedia.org). Histological images B), D), F) in linear polarised light and C) and E) in crossed polarised light with additional use of lambda compensator. B, C) Lateral cortex of *Prolagus oeningensis* femur PIMUZ A/V 4532 showing subendosteal Haversian-like bone in the

1561 inner part and parallel-fibred bone in the central and outer part as well as three LAGs. D,
1562 E) Lateral cortex of *Prolagus imperialis* femur RGM.792094 displaying an identical
1563 pattern of bone tissue but five LAGs. F) Outer anterolateral cortex of *Prolagus sardus*
1564 femur NMB Ty.12659 displaying five LAGs. Note that the line in the lower third of the
1565 cortex is a resorption line (RL) and not a LAG. Occurrence of LAGs indicated by white
1566 or yellow arrows.

Table 1(on next page)

Table 1: Material used in this study.

Specimens sampled in this study with ontogenetic stage, geological age, locality of death/fossil site, and specimen number.
Institutional Abbreviations: **CKS** Cyprus Kissonerga collection of the University of Athens; **MTA** Natural History Museum, The General Directorate of Mineral Research and Exploration, Ankara, Turkey; **NMB** Naturhistorisches Museum Basel, Switzerland; **NMING** National Museum of Ireland - Natural History; **NMW** Naturhistorisches Museum Wien, Austria; **OMNH** Osaka Museum of Natural History, Japan; **PIMUZ** Paläontologisches Institut und Museum, Universität Zürich, Switzerland; **RGM** Rijksmuseum voor Geologie en Mineralogie (now Netherlands Centre for Biodiversity Leiden)

Table 1: Material used in this study. Specimens sampled in this study with ontogenetic stage, geological age, locality of death/fossil site, and specimen number.

Species	Object	Ontogenetic stage	Geological age; Locality	Specimen number
Megaloceros giganteus	Tibia	adult	Late Pleistocene; Baunmore Townland, Rep. of Ireland	NMING:F21306/14
Sinomegaceros yabei	Tibia	juvenile	Late Pleistocene; Kumaishi-do Cave, Miyama, Hachiman-cho, Gujo City, Gifu Prefecture, Japan	OMNH QV-4067
"	Tibia	adult	"	OMNH QV-4068
"	Femur	juvenile	"	OMNH M-087
"	Femur	adult	"	OMNH QV-4062
Pudu puda	Femur		Tiergarten Schönbrunn, Vienna, Austria	NMW 60135
Didelphis albiventris	Femur	adult	La Plata, Argentina	PIMUZ A/V 5279
"	"	adult	"	PIMUZ A/V 5277
"	"	adult	Ingeniero Mashwitzt, Argentina	PIMUZ A/V 5276
"	"	adult	Ranchos, Argentina	PIMUZ A/V 5278
Lutreolina crassicautada	"	adult	Mar de Ajo, Argentina	PIMUZ A/V 5275
"	"	adult	La Plata, Argentina	PIMUZ A/V 5274
Hippopotamus minor	"	juvenile	Late Pleistocene; Kissonerga, Cyprus	CKS 110/B
"	"	juvenile	"	CKS 122/B
"	"	subadult	"	CKS 117
"	Tibia	adult	"	CKS 215

Leithia sp.	"	adult	Pleistocene; Grotta di Maras, Sicily	NMB G 2160
Deinogalerix sp.	Femur	adult	Late Miocene; Gervasio 1, Gargano, Italy	RGM.178017
"	Humerus	adult	Late Miocene; Chiro 20E, Foggia, Gargano, Italy	RGM.425360
Mikrotia magna	Femur	adult	Late Miocene; Sono Giovo, Gargano	RGM.792083
"	"	adult	"	RGM.792084
"	"	adult	"	RGM.792085
"	"	adult	"	RGM.792086
Prolagus apricenicus	Femur	adult	Late Miocene; San Giovannino, Gargano	RGM.792087
"	"	adult	"	RGM.792088
"	"	adult	"	RGM.792089
"	"	adult	"	RGM.792090
"	"	adult	"	RGM.792091
"	"	adult	"	RGM.702092
"	Humerus	adult	"	RGM.792093
"	"	adult	"	RGM.792094
"	"	adult	"	RGM.792095
Prolagus imperialis	Femur	adult	"	RGM.792096
"	"	adult	"	RGM.792097
"	"	adult	"	RGM.792098
"	"	adult	"	RGM.792099
"	"	adult	"	RGM.792100
"	"	adult	"	RGM.792101
"	Humerus	juvenile	"	RGM.792102

"	"	adult	"	RGM.792103
"	"	adult	"	RGM.792104
Prolagus sardus	Femur	juvenile	Late Pleistocene; Monte San Giovanni, Sardinia	NMB Ty. 4974
"	"	adult	"	NMB Ty. 4977
"	"	adult	Late Pleistocene; Grotta Nicolai, Sardinia	NMB Ty.12656
"	"	adult	"	NMB Ty.12657
"	"	adult	Late Pleistocene; Isola di Tavolara, Sardinia	NMB Ty.12658
"	"	adult	"	NMB Ty.12659
Prolagus oeningensis	Femur	juvenile	Middle Miocene; La Grive, France	PIMUZ A/V 4532
	"	adult		PIMUZ A/V 4532
"	"	adult	"	PIMUZ A/V 4532
"	Humerus	adult	"	PIMUZ A/V 4532
"	"	adult	"	PIMUZ A/V 4532
Paraceratherium sp.	Rib	adult	Late Oligocene; Gözükizilli, Turkey	MTA-TTM 2006-1209

Institutional Abbreviations: **CKS** Cyprus Kissonerga collection of the University of Athens; **MTA** Natural History Museum, The General Directorate of Mineral Research and Exploration, Ankara, Turkey; **NMB** Naturhistorisches Museum Basel, Switzerland; **NMING** National Museum of Ireland - Natural History; **NMW** Naturhistorisches Museum Wien, Austria; **OMNH** Osaka Museum of Natural History, Japan; **PIMUZ** Paläontologisches Institut und Museum, Universität Zürich, Switzerland; **RGM** Rijksmuseum voor Geologie en Mineralogie (now Netherlands Centre for Biodiversity Leiden)

1

Figure 1: Typical mammalian bone tissue as observed in large mammals such as cervids.

Red bars indicate area and plane of sectioning. Histological images B), E), and I) in linear polarised light, C) in crossed polarised light and with additional use of lambda compensator, and F) in crossed polarised light. A) Life reconstruction of the cervid *Megaloceros giganteus* ("Knight Megaloceros" by Charles R. Knight, courtesy of the American Museum of Natural History via Wikimedia Commons - http://commons.wikimedia.org). B, C) Bone cortex of a tibia of *Megaloceros giganteus* specimen NMING:F21306/14 displaying an endosteal lamellar layer (innermost part of the cortex) and reticular as well as plexiform fibrolamellar primary bone with growth marks. Note that the primary bone is pervaded by secondary Haversian systems in the inner third of the bone cortex. White arrows indicate lines of arrested growth. Occurrence of LAGs indicated by black/white arrows and the outer circumferential layer (OCL) by white brackets. D) Photograph of *Pudu puda* ("Pudupuda hem 8 FdoVidal Villarr 08Abr06-PhotoJimenez", courtesy of Jaime E. Jimenez via Wikimedia Commons - http://commons.wikimedia.org). E, F) Bone cortex of a femur of *Pudu puda* specimen NMW 60135 displaying an endosteal lamellar layer and mainly plexiform fibrolamellar bone. G) Reconstruction of *Paraceratherium* ("Indricotherium11", Courtesy of Dmitry Bogdanov via Wikimedia Commons - http://commons.wikimedia.org). H) Cross-section of a rib of *Paraceratherium* sp. specimen MTA-TTM 2006-1209. Red rectangle indicates area of dense Haversian bone magnified in I).

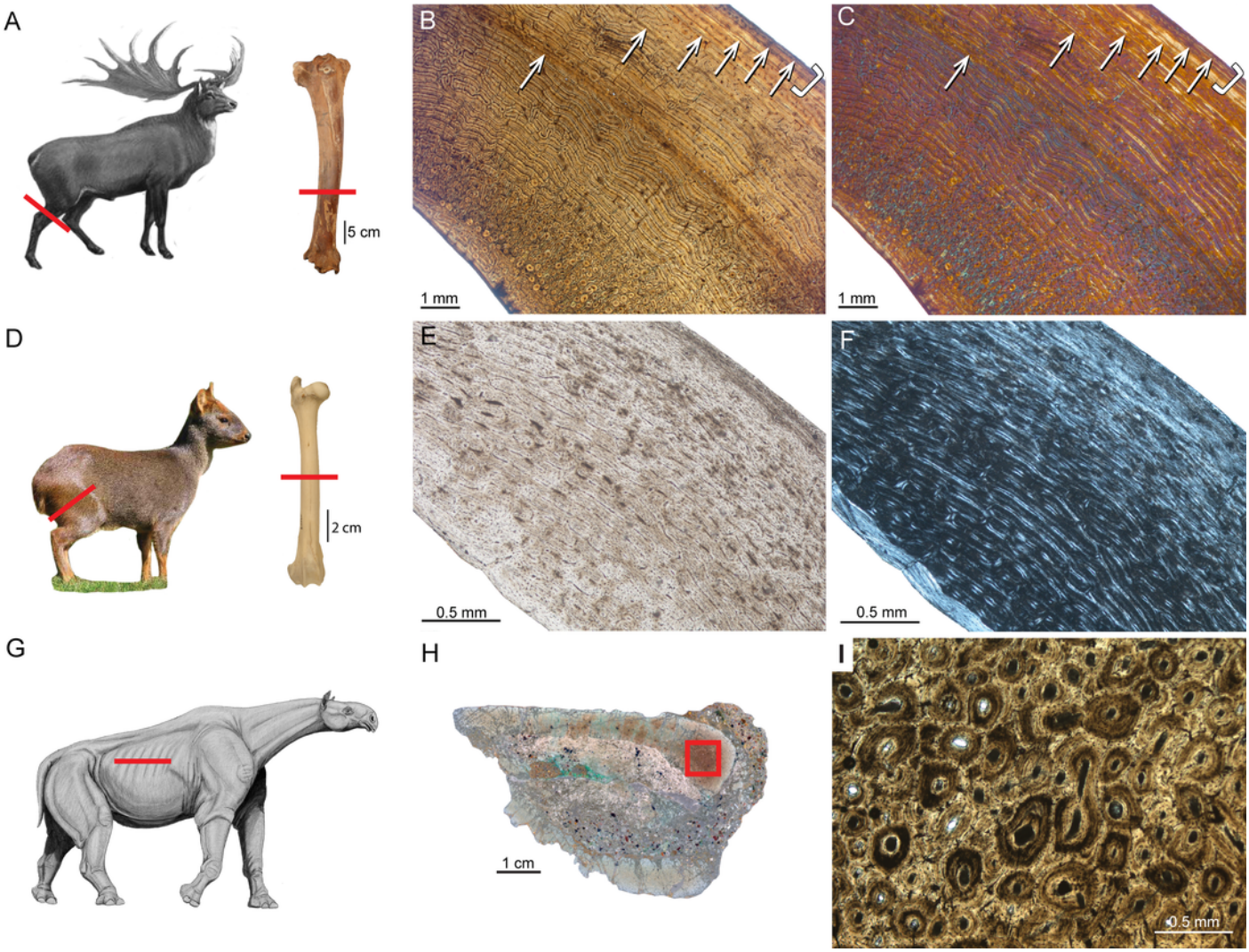
A
5 cm
B
1 mm
C
1 mm
D
2 cm
E
0.5 mm
F
0.5 mm
G
H
1 cm
I
0.5 mm

2

Figure 2: Phylogeny of basal synapsids focussing on groups discussed,

based on Rubidge & Sidor (2001), Benson (2012), and Brink & Reisz (2014).

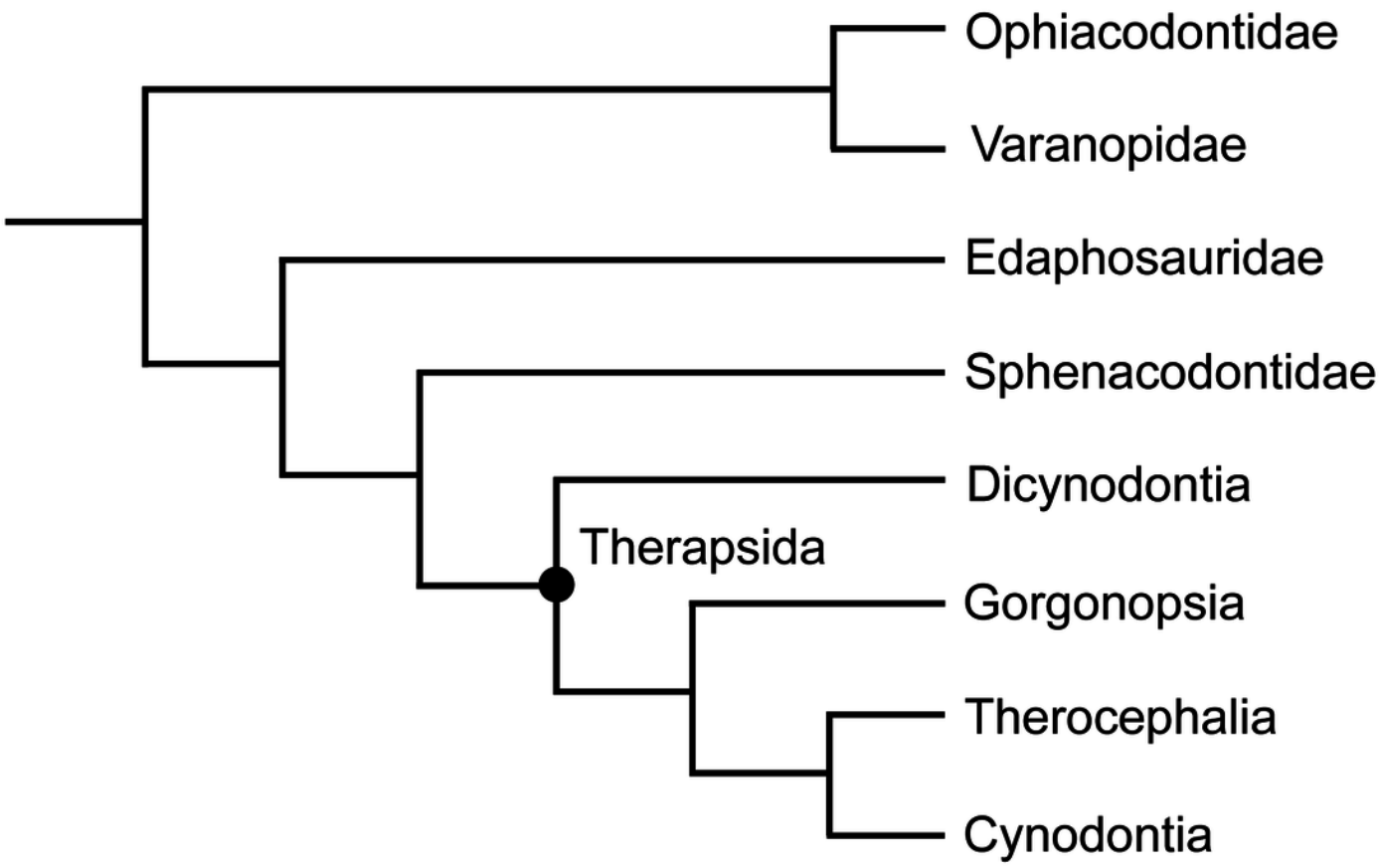

3

Figure 3: Phylogeny of Mammaliamorpha focussing on groups discussed,

based on Luo et al. (2005), Luo et al. (2011), Meredith et al. (2011), and O'Leary et al. (2013). Notoungulates and Pantodonta are not included given their controversial systematic position.

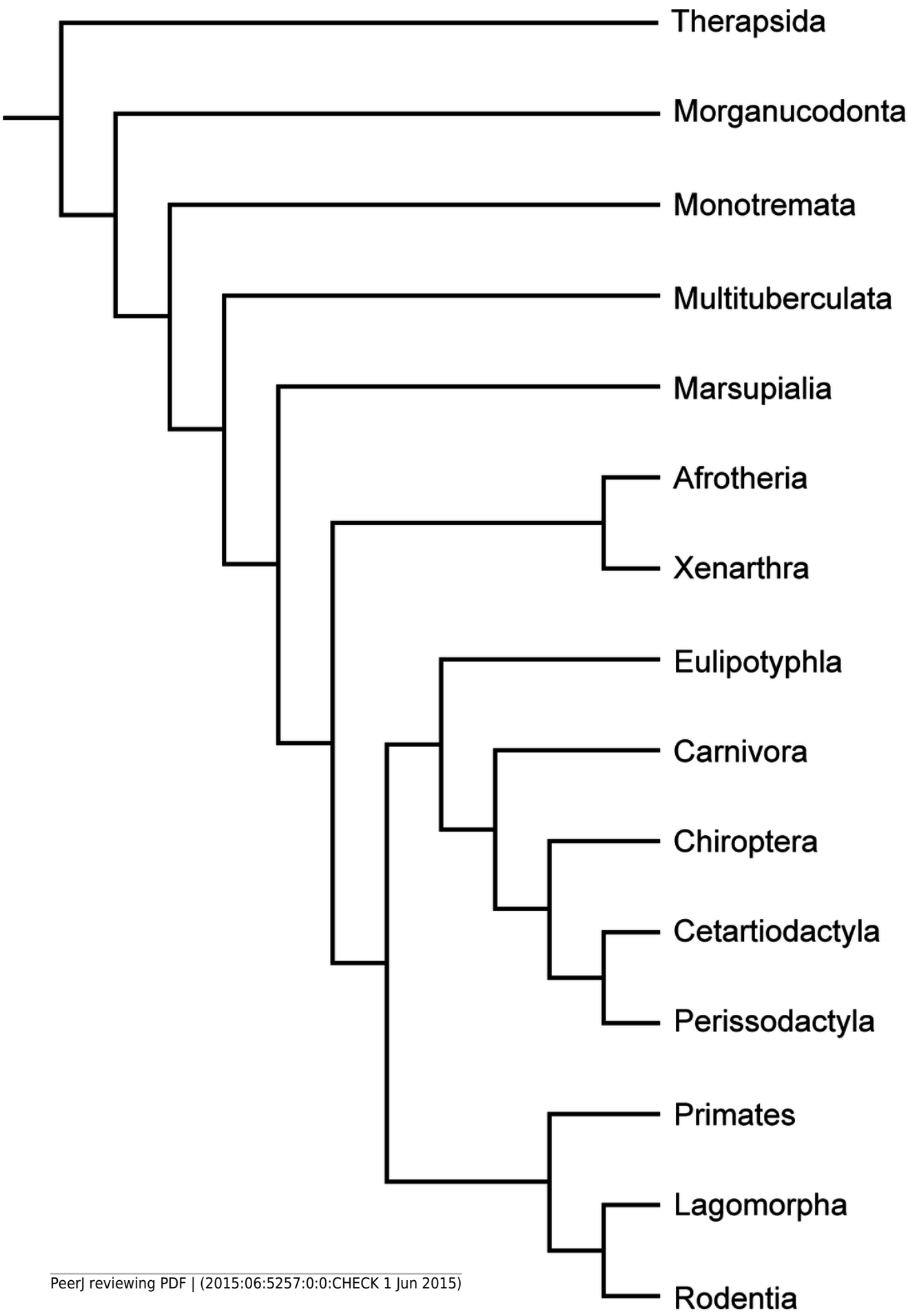
Therapsida
Morganucodonta
Monotremata
Multituberculata
Marsupialia
Afrotheria
Xenarthra
Eulipotyphla
Carnivora
Chiroptera
Cetartiodactyla
Perissodactyla
Primates
Lagomorpha
Rodentia

4

Figure 4: Femoral bone cortex of marsupials.

Histological images A) and D) in linear polarised light and B), C), E), and F) in crossed polarised light. A, B) Outer bone cortex of adult *Didelphis albiventris* specimen PIMUZ A/V 5279. Note the occurrence of simple primary longitudinal vascular canals and primary osteons in mainly parallel-fibred bone tissue. C) Inner bone cortex of the same specimen displaying a distinct endosteal lamellar layer. D, E) Bone cortex of adult *Lutreolina crassicautada* specimen PIMUZ A/V 5275. F) Inner cortex of same specimen. Note the occurrence of primary longitudinal vascular canals and primary osteons as well as Haversian systems within the parallel-fibred bone.

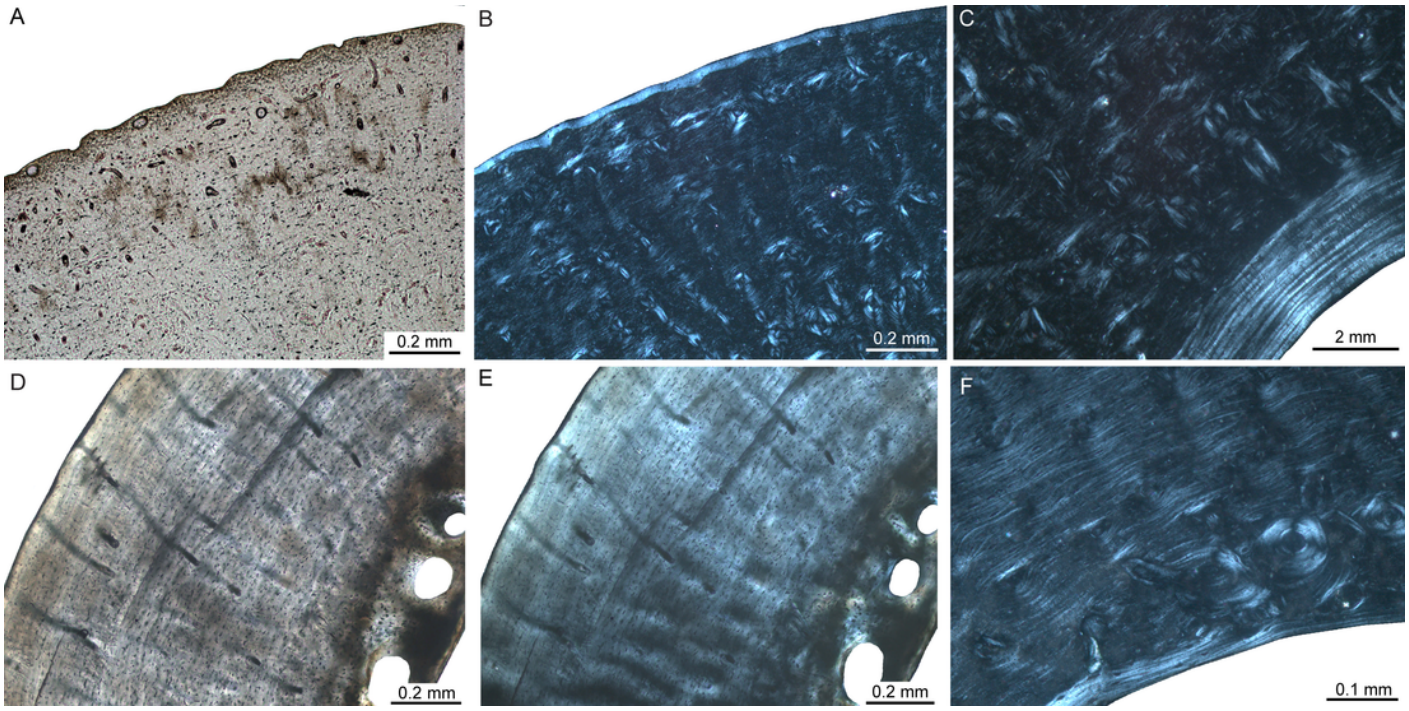

5

Figure 5: Histological features of the femur of *Deinogalerix* sp.

A) Life reconstruction of *Deinogalerix koenigswaldi* in comparison to the extant hedgehog *Erinaceus* (modified from Agustí & Antón, 2002). B) Adult right femur (specimen RGM.178017) in anterior view. Red bar indicates area and plane of sectioning. C) Lateral bone cortex in crossed polarised light showing parallel-fibred bone and 5 LAGs. Occurrence of LAGs indicated by white arrows.

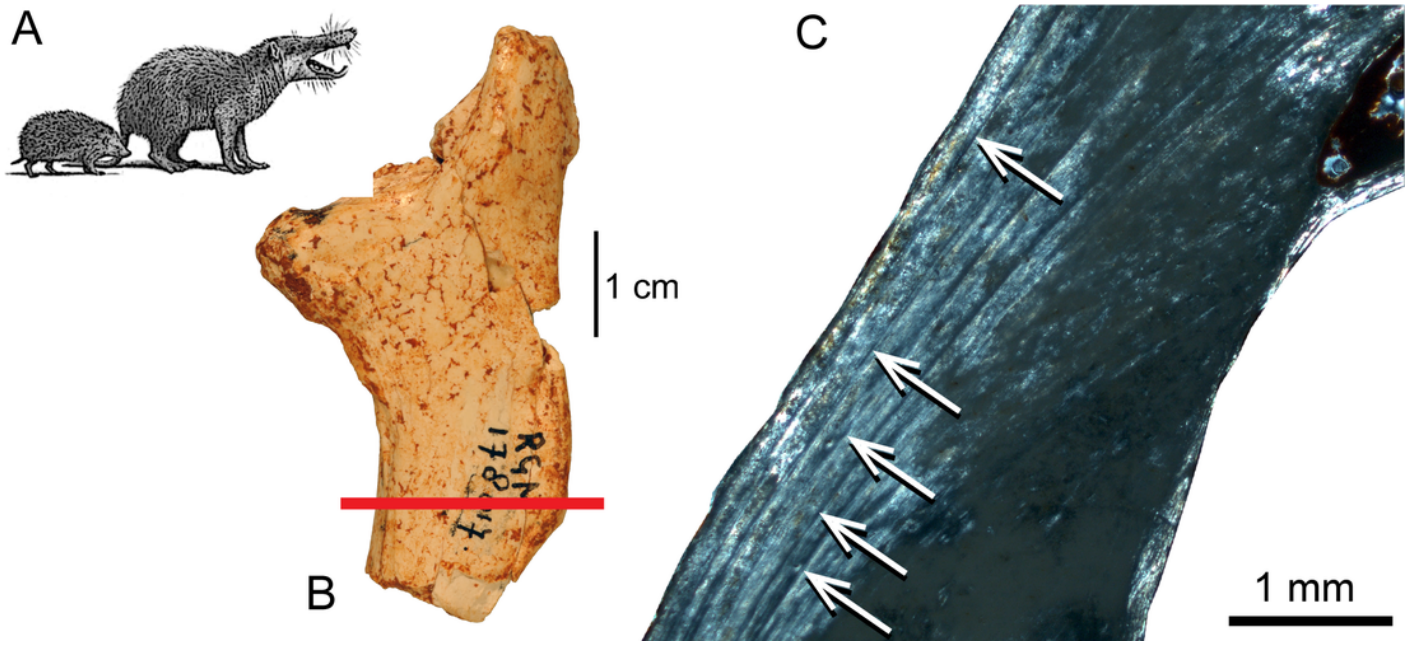

6

Figure 6: Bone cortex of *Hippopotamus minor* femora.

A) Life reconstruction (from van der Geer et al., 2010; drawing: Alexis Vlachos) of another Mediterranean dwarf hippopotamid from the Middle Pleistocene of Crete. Since no life reconstruction of *Hippopotamus minor* is available, we here show the one of *Hippopotamus creutzburgi*. Histological images B), and C) in linear polarised light, D) in crossed polarised light. B) Small juvenile specimen CKS 110/B. C) Intermediate sized juvenile specimen CKS 122/B showing reticular to plexiform vascularised bone. Note that the central part mainly consists of reticular bone. D) Outer bone cortex of large juvenile specimen CKS 117 showing mainly parallel-fibred bone. Black and grey areas indicate zones of recrystallisation due to diagenetic alteration of bone tissue.

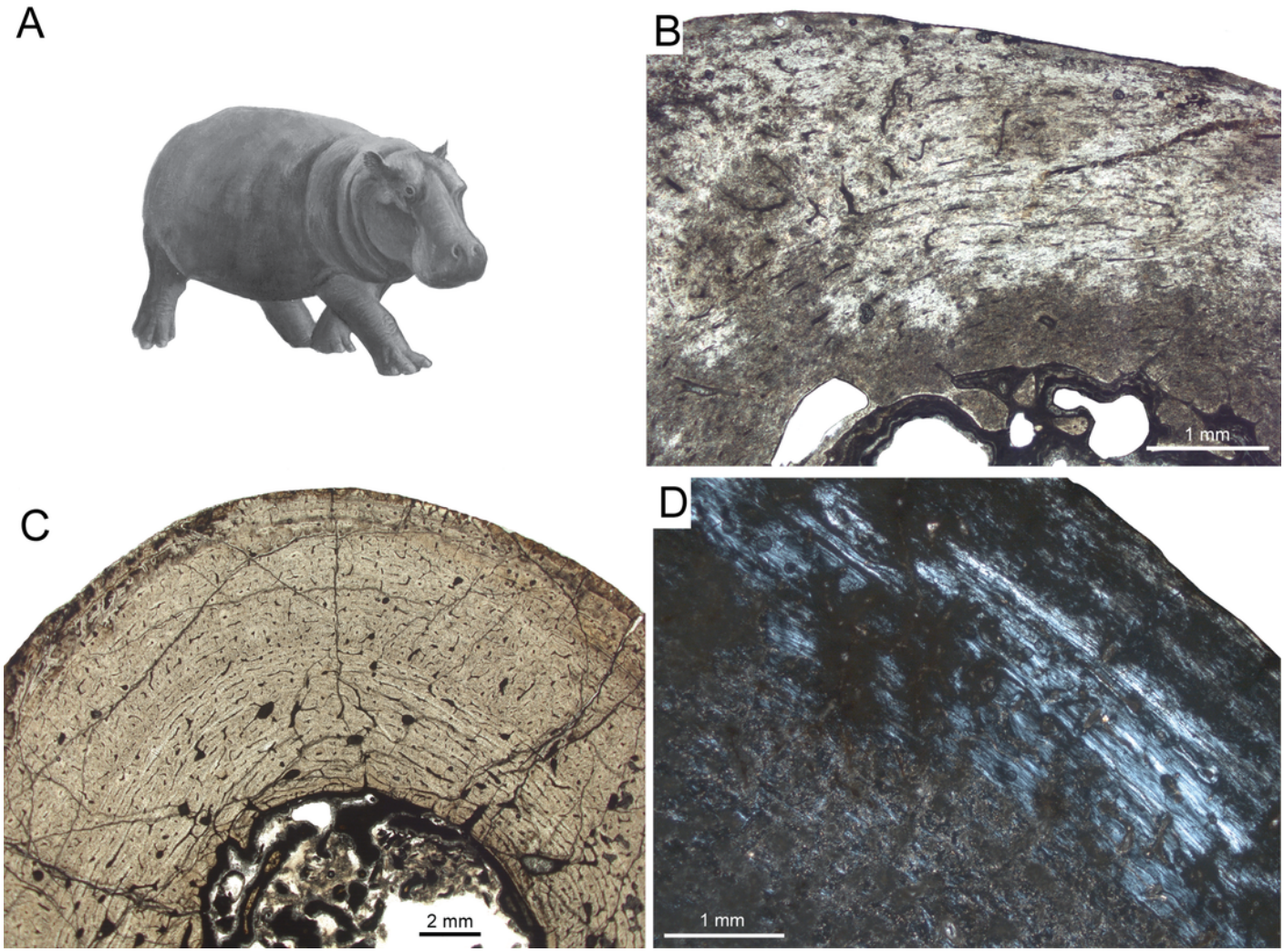
A
B
1 mm
C
2 mm
D
1 mm

7

Figure 7: Histological features of *Sinomegaceros yabei*, the megacerine deer from the Pleistocene of Japan.

Histological images in linear polarised light of an adult femur (OMNH QV-4062) depicting A) the whole cross-section and B) a close-up of the outer cortex. The red bar in A) localizes the approximated position of the section on the life reconstruction (courtesy of Hirokazu Tokugawa), and the red rectangle indicates the area of the close-up. B) Note that seven LAGs are visible, as indicated by white arrows.

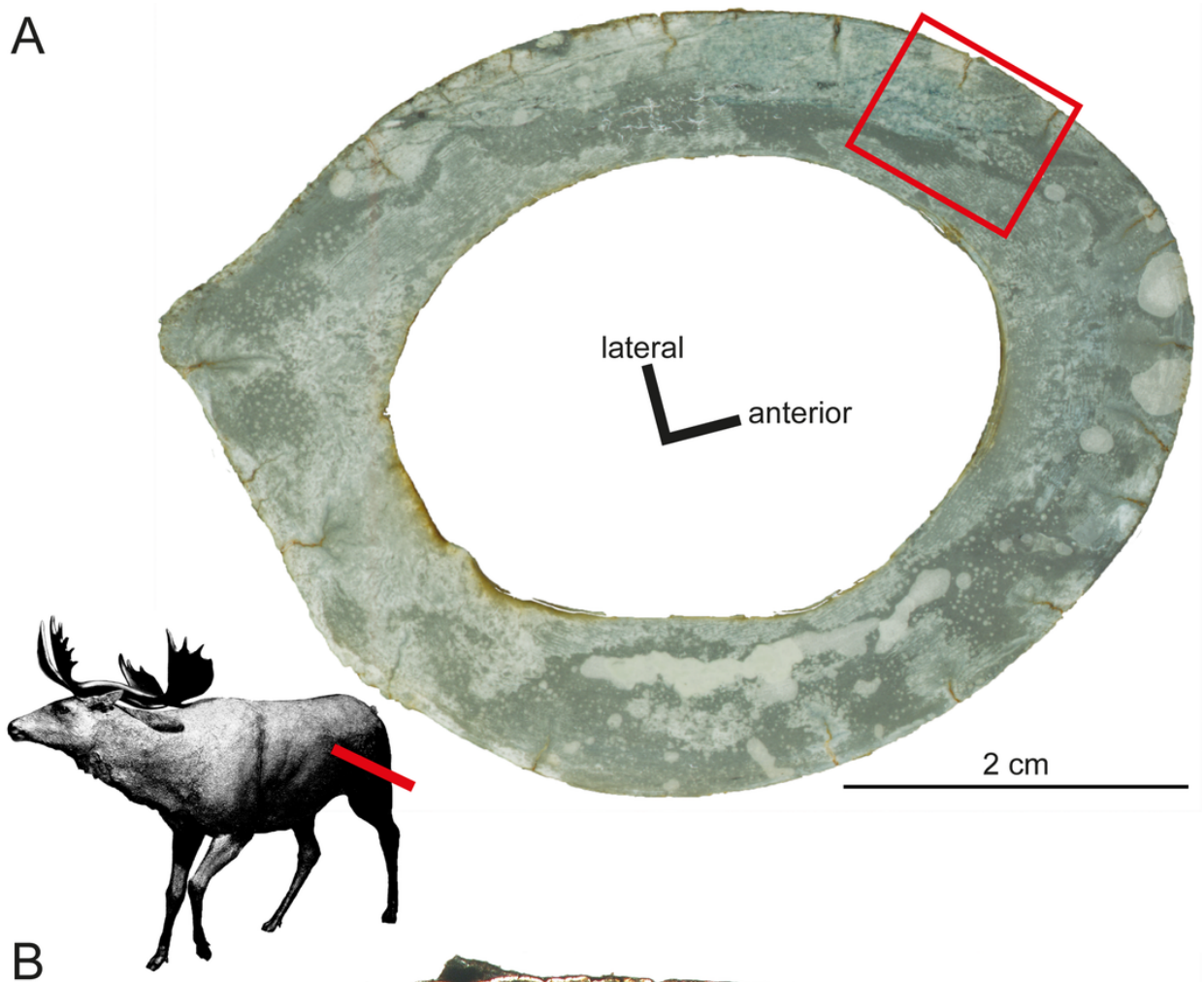
A
lateral
anterior
2 cm

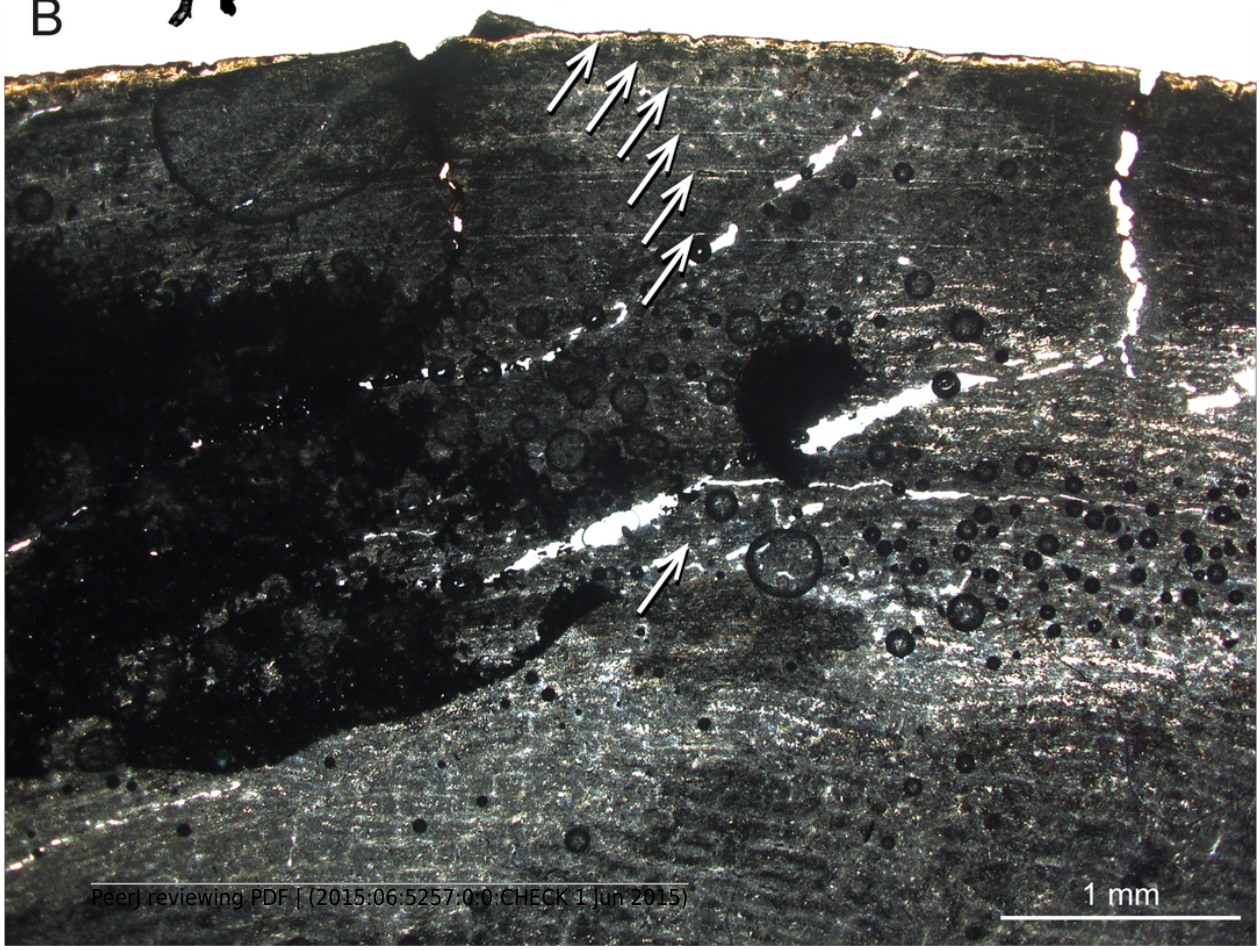
B
1 mm

8

Figure 8: Bone histology of fossil island rodents.

Histological images A) and D) in linear polarised light, B) and E) in crossed polarised light, and C) and F) in crossed polarised light with additional use of lambda compensator. A-C) Adult *Mikrotia* sp. femur (specimen RGM.792085) showing disorganised, parallel-fibred/lamellar bone in its centre. D-F) Adult femur of *Leithia* sp. specimen NMB G 2160 displaying lamellar bone being pervaded by longitudinal to radial primary osteons and irregularly shaped and partially oblique secondary osteons.

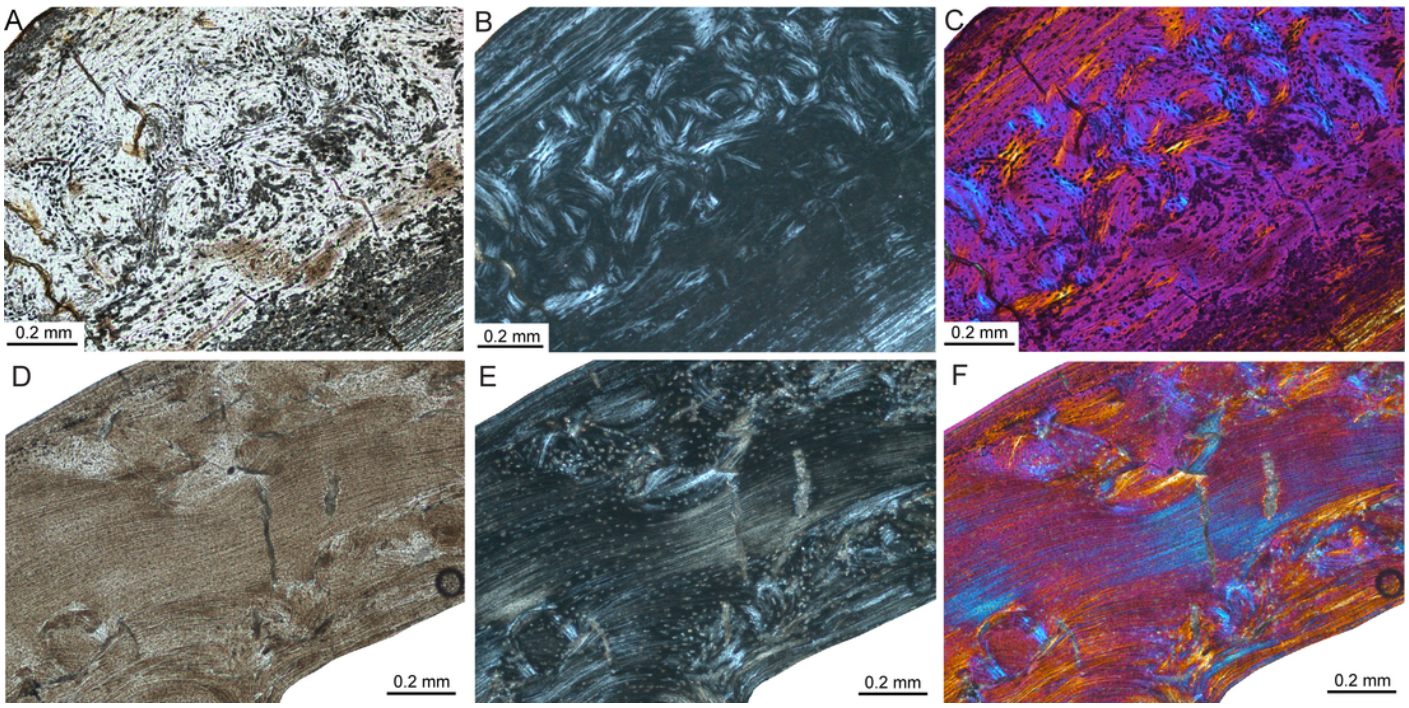

9

Figure 9: Bone histology of fossil ochotonids.

A) Life reconstruction of *Prolagus sardus* ("Prolagus3", courtesy of Wikimedia Commons - http://commons.wikimedia.org). Histological images B), D), F) in linear polarised light and C) and E) in crossed polarised light with additional use of lambda compensator. B, C) Lateral cortex of *Prolagus oeningensis* femur PIMUZ A/V 4532 showing subendosteal Haversian-like bone in the inner part and parallel-fibred bone in the central and outer part as well as three LAGs. D, E) Lateral cortex of *Prolagus imperialis* femur RGM.792094 displaying an identical pattern of bone tissue but five LAGs. F) Outer anterolateral cortex of *Prolagus sardus* femur NMB Ty.12659 displaying five LAGs. Note that the line in the lower third of the cortex is a resorption line (RL) and not a LAG. Occurrence of LAGs indicated by white or yellow arrows.

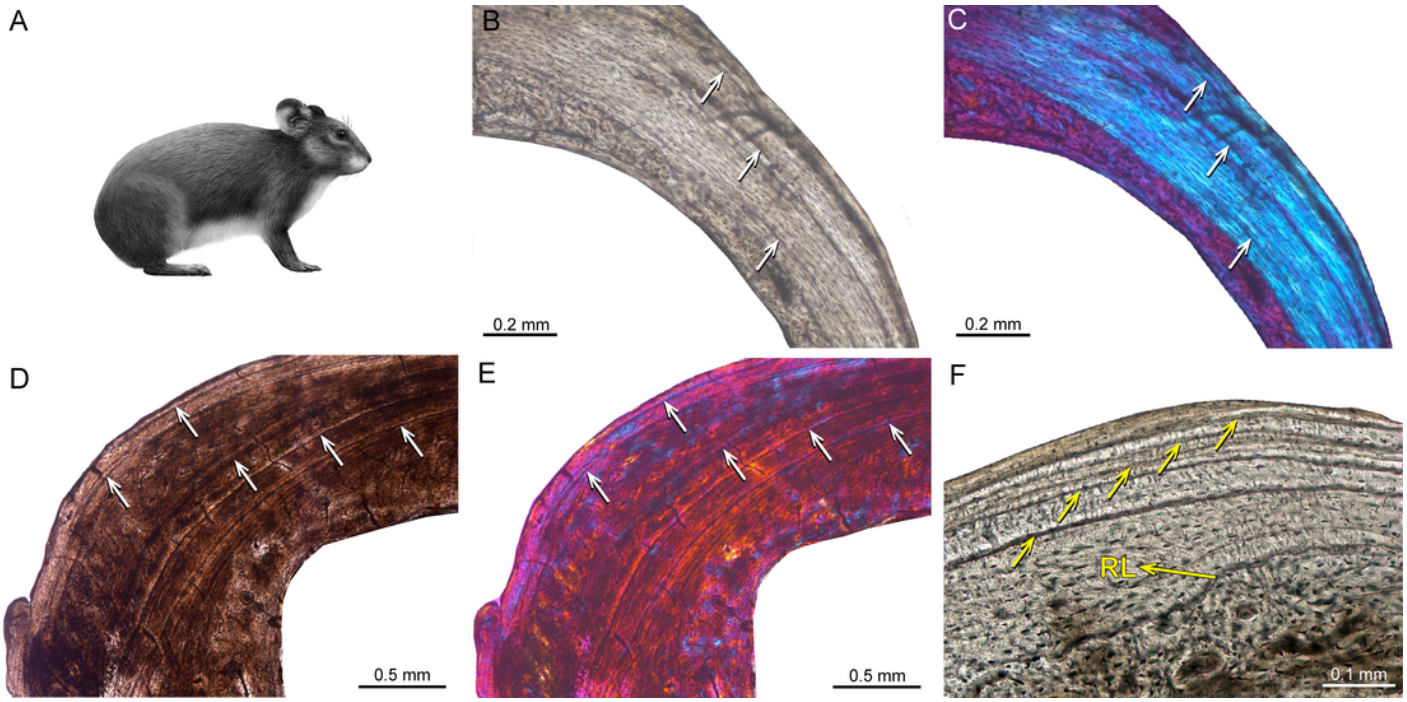

Table 2(on next page)

Table 2: Summary of histological traits of major synapsid clades

(based on material sampled and references cited in the current study). The terminology follows Francillon-Vieillot et al. (1990).

Table 2: Summary of histological traits of major synapsid clades (based on material sampled and references cited in the current study). The terminology follows Francillon-Vieillot et al. (1990).

Histological traits	**Non-therapsid synapsids**	**Non-mammalian therapsids**	**Multitubercula-tes and early mammals**	**Monotremata**	**Euarchontogli-res**	**Laurasiatheria**	**Afrotheria**	**Xenarthra**
Main primary bone tissue types	fibrolamellar, parallel-fibred, lamellar	fibrolamellar	fibrolamellar, parallel-fibred, lamellar	fibrolamellar, lamellar	lamellar or parallel-fibred	fibrolamellar	fibrolamellar	fibrolamellar
Main vascularisation patterns	longitudinal, reticular, radial	plexiform, laminar, longitudinal, reticular, radial	longitudinal, radial, reticular	longitudinal, radial, reticular, circular	longitudinal, reticular, radial	longitudinal, reticular, radial, laminar, plexiform	circumferential, longitudinal, reticular, laminar, plexiform	longitudinal, reticular, radial
Lines of arrested growth	present	present	present	not documented	present	present	present	present
Remodelling	Haversian bone	Haversian bone	not documented	Haversian bone	Haversian bone; rodents: low content of Haversian systems	Haversian bone	Haversian bone	Haversian bone